SIMULATION AND VALIDATION OF VAPOR COMPRESSION SYSTEM

FAULTS AND START-UP/SHUT-DOWN TRANSIENTS

A Thesis

by

BALAKRISHNA AYYAGARI

Submitted to the Office of Graduate Studies of
Texas A&M University
in partial fulfillment of the requirements for the degree of

MASTER OF SCIENCE

August 2011

Major Subject: Mechanical Engineering

Simulation and Validation of Vapor Compression System Faults and Start-Up/Shut-

Down Transients

SIMULATION AND VALIDATION OF VAPOR COMPRESSION SYSTEM

FAULTS AND START-UP/SHUT-DOWN TRANSIENTS

A Thesis

by

BALAKRISHNA AYYAGARI

Submitted to the Office of Graduate Studies of
Texas A&M University
in partial fulfillment of the requirements for the degree of

MASTER OF SCIENCE

Approved by:

Chair of Committee,	Bryan Rasmussen
Committee Members,	Jorge Alvarado
	Michael Pate
Head of Department,	Dennis O'Neal

August 2011

Major Subject: Mechanical Engineering

ABSTRACT

Simulation and Validation of Vapor Compression System Faults and Start-up/Shut-down
Transients.

(August 2011)

Balakrishna Ayyagari, B.Tech., Mahatma Gandhi Institute of Technology, India

Chair of Advisory Committee: Dr. Bryan P. Rasmussen

The statistics from the US Department of Energy show that about one-third of the total consumption of electricity in the households and industries is due to the Air Conditioning and Refrigeration (AC&R) systems. This wide usage has prompted many researchers to develop models for each of the components of the vapor compression systems. However, there has been very little information on developing simulation models that have been validated for the conditions of start-up/shutdown operations as well as vapor compression system faults. This thesis addresses these concerns and enhances the existing modeling library to capture the transients related to the above mentioned conditions.

In this thesis, the various faults occurring in a vapor compressor cycle (VCC) have been identified along with the parameters affecting them. The transients of the refrigerant have also been studied with respect to the start-up/shutdown of a vapor compression system. All the simulations related to the faults and start-up/shutdown have been performed using the vapor compression system models developed in

MATLAB/Simulink environment and validated against the 3-ton air conditioning unit present in the Thermo-Fluids Control Laboratory at Texas A&M University.

The simulation and validation results presented in this thesis can be used to lay out certain rules of thumb to identify a particular fault depending on the unusual behavior of the system thus helping in creating certain fault diagnostic algorithms and emphasize the importance of the study of start-up/shutdown transient characteristics from the point of actual energy efficiency of the systems. Also, these results prove the capability and validity of the finite control volume models to describe VCC system faults and start-up/shutdown transients.

DEDICATION

To my parents and friends

ACKNOWLEDGEMENTS

I would like to thank my thesis advisor, Dr. Bryan Rasmussen, and committee members, Dr. Jorge Alvarado and Dr. Michael Pate, for their continuous guidance and support over the course of this research work. I would like to acknowledge the insight and encouragement provided by Dr. Rasmussen without which this research would not have been possible. I would like to extend my thanks to all my colleagues: Matt Elliot, Swarooph, Bhaskar, Alex, and Nataraj, for their valuable suggestions and also maintain a lighter laboratory atmosphere by holding enlightening conversations. I would like to thank my parents for their constant support and belief in my thoughts without which this would not have been possible. Finally, I am grateful to all my friends who have made my stay in College Station a memorable experience.

NOMENCLATURE

$HVAC\&R$	Heating, Venting, Air Conditioning and Refrigeration
VCC	Vapor Compression Cycle
$AC\&R$	Air Conditioning and Refrigeration
A_i	Internal surface area of heat exchanger
A_o	External surface area of heat exchanger
C_d	Coefficient of Discharge of the expansion valve
EEV	Electronic Expansion Valve
E_w	Heat exchanger tube wall energy
FCV	Finite Control Volume
h	Enthalpy of the refrigerant
H	Energy due to refrigerant flow
MB	Moving Boundary
$\dot{m}_{air}$	Mass flow rate of the air over the evaporator
$\dot{m}_{in}$	Mass flow rate of the refrigerant flowing into the evaporator
$\dot{m}_k$	Mass flow rate of the refrigerant flowing through the compressor
$\dot{m}_{out}$	Mass flow rate of the refrigerant flowing out of the evaporator
$\dot{m}_v$	Mass flow rate of the refrigerant flowing through the valve
P	Pressure
P_c	Condenser pressure
P_e	Evaporator pressure

P_{in}	Pressure at expansion valve inlet
P_{out}	Pressure at expansion valve outlet
Q_a	Energy due to heat transfer between heat exchanger tube wall and air
Q_w	Energy due to heat transfer between refrigerant and heat exchanger tube wall
T_a	Temperature of air
T_r	Temperature of the refrigerant
T_w	Temperature of heat exchanger tube wall
U	Refrigerant Energy
u	Internal energy of the refrigerant
u_v	Percentage opening of the EEV
V_k	Volume of the compressor
W	Instantaneous work input to the system
Gr	Grashoff's number
g	Acceleration due to gravity
T_w	Wall temperature
T_{sat}	Saturation temperature
L	Length of heat exchanger
$\dot{m}$	Mass flow rate of air
Nu	Nusselt's number
Pr	Prandlt number

h_{conv} Free convection heat transfer coefficient

h_{cond} Film wise condensation heat transfer coefficient

k Thermal conductivity of liquid

h_{fg} Enthalpy of the vaporization

d Diameter of the tube

F Two phase multiplier for heat transfer

h_{nb} Pool boiling (Nucleate boiling) heat transfer coefficient

h_{cb} Convective boiling heat transfer coefficient

R Convection reduction parameter

Re_l Liquid alone Reynold's number

X_{tt} Lockhart-Martinelli parameter

q Heat flux

Fr_l Liquid Froude number

h_l Liquid alone heat transfer coefficient

M Molecular weight

V Velocity of air

F_v Fan voltage

A Area through which the air exits

Re Reynolds number

D_h Hydraulic diameter

C_p Specific heat of air

k_a	Thermal conductivity of air
G	Mass flux
j_h	Colburn j-factor

Greek symbols

α_i	Heat transfer coefficient between refrigerant and heat exchanger tube wall
α_o	Heat transfer coefficient between heat exchanger tube wall and air
ΔP	Pressure differential across the valve
ρ	Density of the refrigerant
ρ_w	Density of heat exchanger tube wall material
η_a	Adiabatic efficiency of the compressor
η_k	Volumetric efficiency of the compressor
ρ_k	Density of refrigerant at compressor inlet
ω_k	Compressor speed in rotations per second
μ_a	Dynamic viscosity of air
ϑ	Volume flow rate
ν	Viscosity
ρ_a	Density of air

TABLE OF CONTENTS

LIST OF FIGURES

LIST OF TABLES

1. INTRODUCTION

A typical US household spends about $1300 on their yearly energy bills according to the US Department of Energy (www.energy.gov) of which 56% is used for heating and cooling the house [1]. Heating, Venting, Air Conditioning and Refrigeration (HVAC&R) systems consume about 40% of the total energy [2]. With the increasing demand for energy, there is a need to develop dynamic models of these systems to study their transient behavior in order to improve their efficiency.

The vapor compression cycle (VCC) is the most widely used method for Air-Conditioning and Refrigeration (AC&R) applications. Although there have been lot of models developed for vapor compression system components to predict the behavior of the system, there is relatively little literature concerning the simulation and validation of these models for a start-up/shutdown condition as well as for those involving soft faults. This analysis is very important considering the fact that most VCC systems operate in a mode by the start and stop of the refrigerant flow to achieve the required heating or cooling.

This thesis lays emphasis on the simulation and validation of the start-up/shutdown transients and the various faults arising in Vapor Compression system. The simulation results are achieved using the Finite Control Volume (FCV) approach of the heat exchangers along with static compressor and valve models. The experimental tests were conducted on the 3-ton residential air conditioning unit from Trane present in the

---

This thesis follows the style of *IEEE Transactions on Automatic Control.*

Thermo-Fluids Control Laboratory at Texas A&M University. The remainder of this section emphasizes on the various components of a vapor compression system and its working.

1.1 Background

A single state vapor compression system consists of the following components: Compressor, Condenser, Expansion Valve and Evaporator.
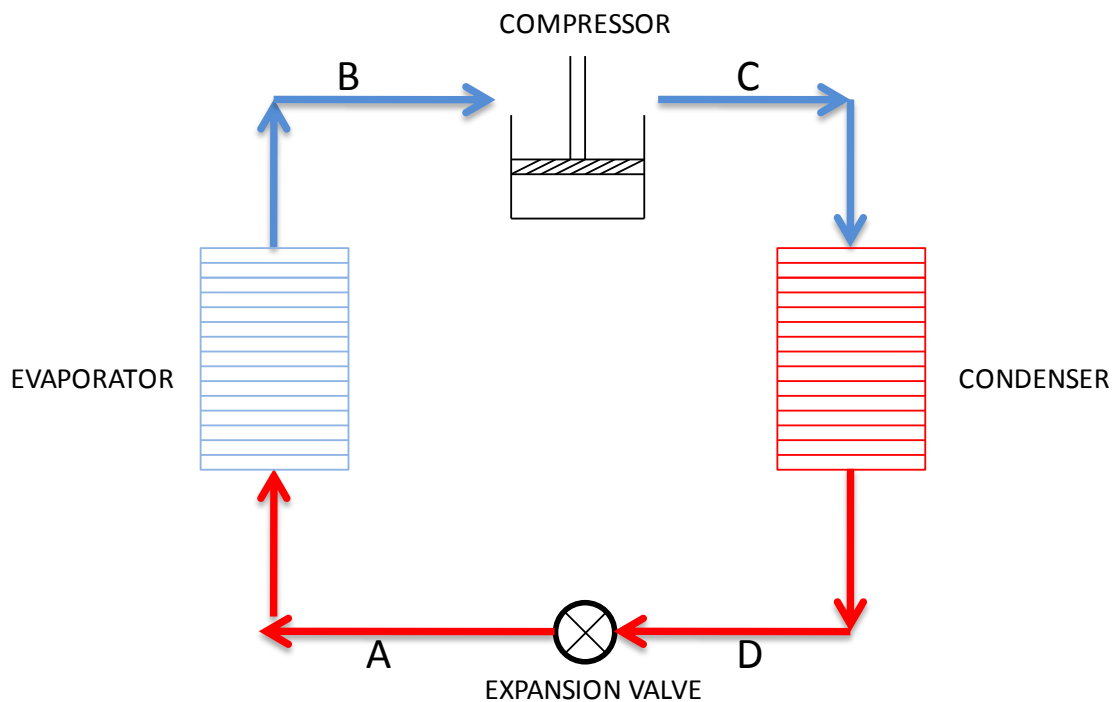
Figure 1.1 Simple Vapor Compression System

The schematic diagram of the vapor compression cycle is shown in the Figure 1.1. In Figure 1.1, the process from B→C through the compressor is an isotropic compression,

process C→D through the condenser takes place at constant pressure, D→A through the valve is an isenthalpic process and A→B through the evaporator occurs at constant pressure.

The operation of the cycle is as follows: the low temperature low pressure vapor at state B (superheated vapor) is compressed by a compressor to a high temperature and pressure vapor at state C (single phase superheated vapor). This vapor is condensed into high pressure at state D (saturated or sub cooled liquid) in the condenser and then passes
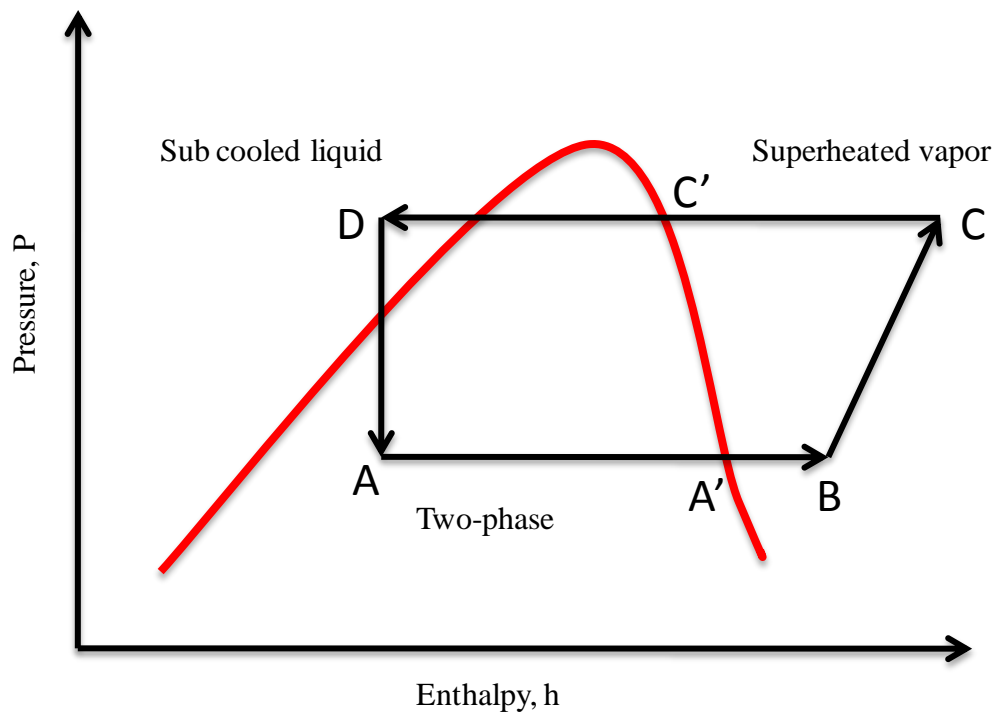
Figure 1.2 P-h Diagram of a Vapor Compression System

through the expansion valve. The liquid refrigerant expands and cools down as it passes from high pressure to low pressure region through the expansion valve at state A

(refrigerant is in two phase). From here, the refrigerant is passed on to an evaporator, where it absorbs heat from the surroundings from the circulating fluid (being refrigerated) and vaporizes into low pressure vapor at state B. The cycle then repeats. The cycle of operation is shown in Figure 1.2. The exchange of energy is as follows:

- Compressor requires work, δW. The work is supplied to the system from the surroundings.

- During condensation, heat $\delta Q1$ the equivalent of latent heat of condensation etc, is lost from the refrigerator.

- During evaporation, heat $\delta Q2$ equivalent to latent heat of vaporization is absorbed by the refrigerant.

- There is no exchange of heat during throttling process through the expansion valve as this process occurs at constant enthalpy.

1.2 Organization of the Thesis

The rest of the thesis is organized as follows: Section 2 presents the modeling of the condenser, evaporator, compressor and expansion valve. Section 3 talks about the experimental system used for validation. Section 4 deals with the simulation and experimental results related to the faults in vapor compression systems. The simulation and validation results for the start-up and shutdown transients are dealt with in Section 5. Section 6 provides the conclusion and future scope of the research.

2. MODELING

The system behavior during start-up, feedback control and potentially during shutdown can be predicted by developing dynamic system models for each of the components in a simple vapor compression system. Fluid flow through the heat exchangers involves one or more transition of fluid phase from vapor to single-phase and vice versa and modeling this behavior is not only difficult but mathematically complex [3] when compared to the modeling of compressor and valve. The rest of this section is organized as follows: Subsection 2.1 deals with the literature review related to modeling; Subsection 2.2 presents the modeling assumptions and Subsections 2.3-2.6 deal with the basic Equations related to each of the vapor compression system components.

2.1 Literature Review

There are two popular approaches that can be followed while modeling the heat exchangers in a vapor compression system namely Finite Control Volume (FCV) and Moving Boundary (MB). Bendapudi [4] compared the two modeling techniques and concluded that the more complex FCV models accurately capture the various transient trends of the system parameters; while the simpler MB approach uses effective parameter values to create a more control-oriented model. Since the validation of start-up/shutdown and fault analysis involves capturing the various transient trends perfectly, this thesis mainly concentrates on the FCV approach. Hemami and Dunn [5] developed a transient model to predict the behavior of a vapor compression cycle of a mobile air-conditioning system. The heat exchangers have been modeled using the FCV approach

while the orifice-tube and compressor models have been developed using the semi-empirical approach. They validated the model with steady state which predicts most of the system parameters to ±15%. Extensive modeling using the FCV approach has been carried out by Abhishek Gupta [3]. Modeling the transient analysis of refrigeration systems has been carried out by Dhar as part of his doctoral thesis [6]. The refrigeration cycle simulation model was developed using the MB approach. This model has been validated against the various dynamic characteristics of the system for different system and experimental conditions. Gruhle and Isermann [7] developed a theoretical model of an evaporator along with the expansion valve and compressor. The evaporator has been modeled using the lumped parameter approach and a suitable controller has been designed for superheat control. Chi and Didion [8] also presented a transient model that followed a lumped parameter approach. Data taken from a 4-ton air to air heat pump was used to validate the model. MacArthur and Grald [9] performed an experimental validation of their distributed parameter dynamic model of vapor compression heat pumps and achieved a good agreement between the model and the experiment. Mithraratne [10] also developed a distributed parameter based numerical model of an evaporator controlled by a thermostatic expansion valve. Wedekind and Bhatt [11] modeled the evaporator and condenser assuming a time-invariant approach of the mean void fraction of the system. Validation results have been provided for a class of transient flow problems where complete vaporization or condensation takes place which depicts the accuracy of the model for those conditions.

2.2 Modeling Assumptions

There have been several assumptions made to simplify the subsequent development of the models of a vapor compression system. Firstly, the heat exchangers are assumed to be dynamic models while the compressor and the expansion valve are modeled using static relationships. This assumption is valid considering the fact that the dynamics of the refrigerant for compressor and expansion valve are much faster than those for the heat exchangers. Secondly, the refrigerant flow inside the heat exchanger can be modeled as a one-dimensional fluid flow by assuming the heat exchanger to be a single long horizontal tube. In an actual experimental system, the turbulence phenomenon leads to three-dimensional refrigerant flow which has an effect on the convective heat transfer coefficient from the refrigerant to the tube. This effect can be nullified by assuming a heat transfer coefficient correlation that can effectively capture the turbulence effects [3]. Thirdly, the pressure drop due to change in the momentum of refrigerant along the length of the heat exchanger is assumed to be negligible. This assumption excludes the use of the Equations related to the conservation of momentum. Finally, the valve is modeled on the concept of isenthalpic expansion while the compressor is modeled on the concept of isentropic compression.

2.3 Evaporator

The FCV modeling approach of the evaporator begins with dividing the evaporator model into *n* control volumes with each of the control volumes following a lumped parameter approach. The model approximates the distributed parametric

scenario by increasing the number of control volumes thus reducing the modeling error (Figure 2.1).
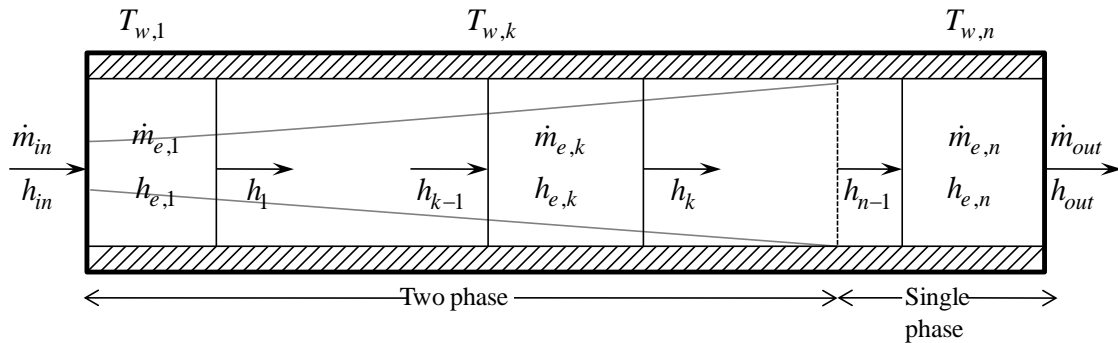
Figure 2.1 FCV Evaporator Model Diagram [3]

The governing ordinary differential Equations are obtained by applying the conservation of refrigerant energy, tube wall energy and mass over each control volume along with the assumptions enlisted in Subsection 2.1.

As can be seen from Figure 2.1, the evaporator consists of two regions: two-phase at the entrance of the evaporator and superheated (single phase) at the exit of the evaporator. For the purpose of modeling, it has been assumed that there is a change of phase of the refrigerant from two-phase to single phase (Figure 2.1). The phase of a refrigerant in any control volume is determined by the outlet enthalpy of the refrigerant in that region. If the outlet enthalpy is less than or equal to the saturated vapor enthalpy, then the refrigerant is said to be in two phase. If the outlet enthalpy is more than the saturated vapor enthalpy, then the state of the refrigerant is single phase (superheated vapor).

In Figure 2.1, $\dot{m}_{in}, h_{in}$ and $\dot{m}_{out}, h_{out}$ are the mass flow rate and enthalpy of the refrigerant at the inlet and exit of the heat exchanger. $\dot{m}_{k-1}, h_{k-1}$ and $\dot{m}_k, h_k$ are the mass flow rate and enthalpy of the refrigerant at the inlet and outlet of the kth control region. $\dot{m}_{e,k}$ gives the rate of change of refrigerant mass and $h_{e,k}$ is assumed to be the average enthalpy in the kth control region of the heat exchanger. Following Subsections briefly describe the conservation Equations required to model the evaporator. A more detailed analysis regarding the derivation of these Equations can be got from [3].

2.2.1 Conservation of Refrigerant Energy

The rate at which the refrigerant energy changes in a system is given by Equation 2.1. Here, $\dot{H}_{in}$ is the rate of energy into the region due to refrigerant flow, $\dot{H}_{out}$ is the rate of energy leaving the region due to refrigerant flow and $\dot{Q}_w$ is the rate of energy due to heat transfer between the refrigerant and the tube wall. At a point the rate of energy due to refrigerant flow is given by Equation 2.2 where $\dot{m}$ is the refrigerant mass flow rate and h is the refrigerant enthalpy at that point. The rate at which the heat energy is transferred to the tube wall is given by Equation 2.3 where α_i is the lumped parameter heat transfer coefficient between the fluid and the tube wall, T_w and T_r are the lumped parameter tube wall and refrigerant temperatures. Equation 2.4 gives the conservation of refrigerant energy for all the control regions.

$$\dot{U} = \dot{H}_{in} - \dot{H}_{out} + \dot{Q}_w \qquad\qquad 2.1$$

$$\dot{H} = \dot{m} \,.\, h \qquad\qquad 2.2$$

$$\dot{Q}_w = \alpha_i A_i (T_w - T_r) \tag{2.3}$$

$$\begin{bmatrix} \dot{U}_1 \\ \vdots \\ \dot{U}_k \\ \vdots \\ \dot{U}_n \end{bmatrix} = \begin{bmatrix} \dot{m}_{in} h_{in} - \dot{m}_1 h_1 + \alpha_{i,1} A_{i,1} (T_{w,1} - T_{r,1}) \\ \vdots \\ \dot{m}_{k-1} h_{k-1} - \dot{m}_k h_k + \alpha_{i,k} A_{i,k} (T_{w,k} - T_{r,k}) \\ \vdots \\ \dot{m}_{n-1} h_{n-1} - \dot{m}_{out} h_{out} + \alpha_{i,n} A_{i,n} (T_{w,n} - T_{r,n}) \end{bmatrix} \tag{2.4}$$

2.2.2 Conservation of Refrigerant Mass

The conservation of refrigerant mass is achieved by taking the difference between the amount of refrigerant entering the region and the amount leaving it. The conservation of refrigerant mass for all regions is given by Equation 2.5. These can be composed into a single Equation by adding them to give Equation 2.13 where, $\dot{m}_{in}$ and $\dot{m}_{out}$ are the mass flow rates of the refrigerant entering and exiting the heat exchanger.

$$\begin{bmatrix} \dot{m}_{e,1} \\ \vdots \\ \dot{m}_{e,k} \\ \vdots \\ \dot{m}_{e,n} \end{bmatrix} = \begin{bmatrix} \dot{m}_{in} - \dot{m}_1 \\ \vdots \\ \dot{m}_{k-1} - \dot{m}_k \\ \vdots \\ \dot{m}_{n-1} - \dot{m}_{out} \end{bmatrix} \tag{2.5}$$

$$\dot{m}_e = \dot{m}_{in} - \dot{m}_{out} \tag{2.6}$$

2.2.3 Conservation of Tube Wall Energy

Equation 2.7 gives the rate of change of tube wall energy where, $\dot{Q}_a$ is the rate of heat transfer between the tube wall and the external fluid. $\dot{Q}_a$ is given by Equation 2.8 where, α_o is the lumped parameter heat transfer coefficient between the tube wall and

the external fluid. A_o is the outside surface area and T_a is the lumped parameter external fluid temperature for each region. The conservation of tube wall energy for all regions, given by Equation 2.9, is achieved by substituting the necessary terms in to Equation 2.7.

$$\dot{E}_w = \dot{Q}_a - \dot{Q}_w \tag{2.7}$$

$$\dot{Q}_a = \alpha_o A_o (T_a - T_w) \tag{2.8}$$

$$\begin{bmatrix} \dot{E}_{w,1} \\ \vdots \\ \dot{E}_{w,k} \\ \vdots \\ \dot{E}_{w,n} \end{bmatrix} = \begin{bmatrix} \alpha_{o,1} A_{o,1}(T_{a,1} - T_{w,1}) - \alpha_{i,1} A_{i,1}(T_{w,1} - T_{r,1}) \\ \vdots \\ \alpha_{o,k} A_{o,k}(T_{a,k} - T_{w,k}) - \alpha_{i,k} A_{i,k}(T_{w,k} - T_{r,k}) \\ \vdots \\ \alpha_{o,n} A_{o,n}(T_{a,n} - T_{w,n}) - \alpha_{i,n} A_{i,n}(T_{w,n} - T_{r,n}) \end{bmatrix} \tag{2.9}$$

The derivation of the governing differential Equations is explained in detail in the appendix section. The nonlinear state space form of Equation 2.10 could be used to describe the entire model.

$$Z(x,u) . \dot{x} = f(x,u) \tag{2.10}$$

The elements of the Z- matrix are explained in detail in [3] and are mentioned in the appendix section.

$$f(x,u) = \begin{bmatrix} \dot{m}_{in}(h_{in} - h_1) + \alpha_{i,1} A_{i,1}(T_{w,1} - T_{r,1}) \\ \vdots \\ \dot{m}_{in}(h_{k-1} - h_k) + \alpha_{i,k} A_{i,k}(T_{w,k} - T_{r,k}) \\ \vdots \\ \dot{m}_{in}(h_{n-1} - h_{out}) + \alpha_{i,n} A_{i,n}(T_{w,n} - T_{r,n}) \\ \dot{m}_{in} - \dot{m}_{out} \\ \alpha_{o,1} A_{o,1}(T_{a,1} - T_{w,1}) - \alpha_{i,1} A_{i,1}(T_{w,1} - T_{r,1}) \\ \vdots \\ \alpha_{o,k} A_{o,k}(T_{a,k} - T_{w,k}) - \alpha_{i,k} A_{i,k}(T_{w,k} - T_{r,k}) \\ \vdots \\ \alpha_{o,n} A_{o,n}(T_{a,n} - T_{w,n}) - \alpha_{i,n} A_{i,n}(T_{w,n} - T_{r,n}) \end{bmatrix}_{(2n+1)X1} \tag{2.11}$$

2.4 Condenser

The condenser can be divided into three regions as shown in Figure 2.2: Single phase super heated vapor at the entrance, two phase region in between and a single phase sub cooled liquid at the exit. Similar to the evaporator, we model the FCV condenser by discretizing into *n* control volumes. As stated earlier, the enthalpy at the outlet of a control volume will determine the state of the fluid in that particular control volume. If the outlet enthalpy of the fluid in a region is greater than the vapor saturation enthalpy (at condenser pressure), the state of the fluid is single phase superheated vapor. If the outlet enthalpy of the fluid is less than the vapor saturation enthalpy but greater than the liquid saturation enthalpy (at condenser pressure), the fluid is said to be two phase. If the outlet enthalpy of the fluid is less than the liquid saturation enthalpy, the fluid in that region is said to be in single phase sub cooled liquid state. All the conservation and governing Equations developed for the evaporator model in Subsection 2.3 are still valid for the FCV condenser.
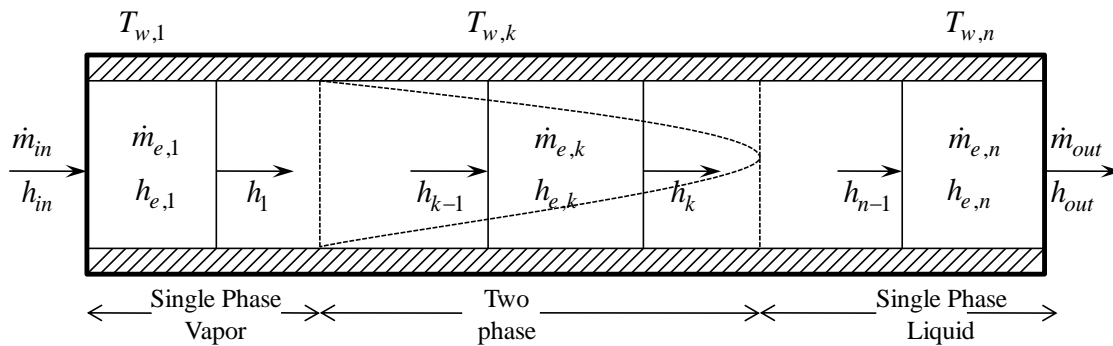
Figure 2.2 FCV Condenser Model Diagram [3]

2.5 Compressor

The modeling of the compressor is done using static relationships. The first of those relationships is used to determine the mass flow rate of the refrigerant at the compressor outlet.

$$\dot{m}_k = \rho V_k \omega_k \eta_k \qquad 2.12$$

where the volumetric efficiency is given by,

$$\eta_k = f_1(\omega_k, \frac{P_{out}}{P_{in}}) \qquad 2.13$$

The second relationship is used to calculate the enthalpy using the assumption of adiabatic compression with an isentropic efficiency η_a. The following are the Equations that describe the relationship.

$$\eta_a = f_2(\omega_k, \frac{P_{out}}{P_{in}}) \qquad 2.14$$

$$h_{out} = \frac{1}{\eta_a}[h_{out,isentropic} + h_{in}(\eta_a - 1)] \qquad 2.15$$

An empirical map is created for η_a and η_k as a function of the pressure ratio and the speed of the compressor.

2.6 Electronic Expansion Valve

The mass flow rate through the electronic expansion valve is modeled based on the following orifice Equation.

$$\dot{m}_v = A_v C_d \sqrt{\rho(P_{in} - P_{out})} \qquad 2.16$$

$$A_v C_d = f_3(u_v, \Delta P) \hspace{4cm} 2.17$$

Here $A_v C_d$ is the discharge coefficient of the valve. It is a semi empirical map that depends on the valve command u_v and the pressure differential across the valve, $\Delta P = P_{in} - P_{out}$. As the valve is assumed to be isenthalpic, enthalpy at the exit of the valve is the same as the enthalpy at its inlet.

$$h_{v,out} = h_{v,in} \hspace{4cm} 2.18$$

The empirical maps for the compressor and valve are created by carrying out experimental analysis to obtain a wide range of condenser and evaporator pressures for various valve positions. The code generating both the compressor and valve map is given in the appendix.

3. EXPERIMENTAL SYSTEM

All the experiments related to start-up/shutdown and faults are conducted on a 3-Ton residential air conditioner unit funded by Trane shown in Figure 3.1. The system is equipped with seven thermocouples to measure the refrigerant and air temperatures at the inlet and exit of the heat exchanger; two pressure sensors to measure the condenser and evaporator pressures; an electronic expansion valve from Parker; two variable speed fans at each of the heat exchangers where the change in the speed of fans will bring about a change in the mass flow rate of the air over the respective heat exchanger; and a two stage fixed scroll compressor. The refrigerant used in the system is R-410A. The schematic of the system showing the placement of various sensors is detailed in Figure 3.2 and the information about the essential components is listed in Table 3.1. Table 3.2 lists the physical parameters of the experimental system. The tuned values are slightly different from the calculated values because of the estimated inner diameter value.

| (a) Evaporator and Air Handler Unit | (b) Compressor and Condenser | (c) DAQ Board and Software |
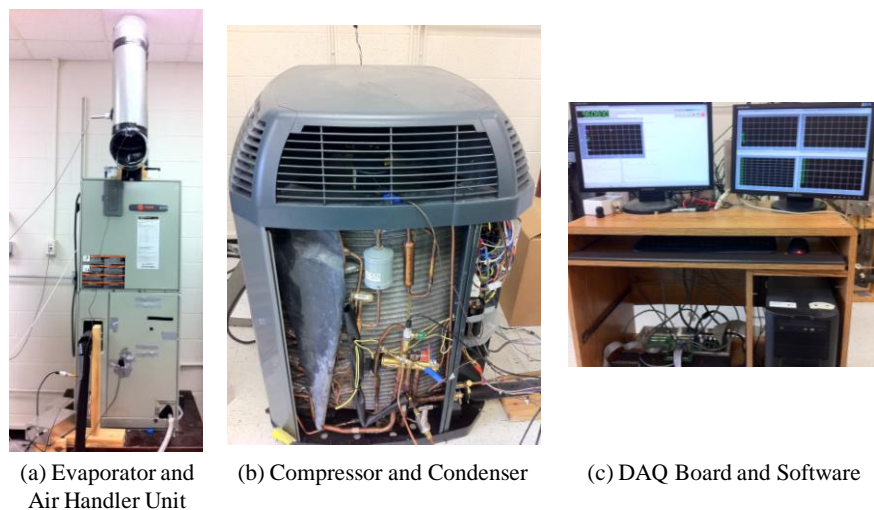
Figure 3.1 3-ton Residential Air Conditioning System

Figure 3.2 Schematic Diagram of the Residential Air Conditioner

Table 3.1 Components of TRANE Experimental System

Component	Manufacturer	Model Number
Air Conditioning System	Trane	XL 16i
EEV	Parker	020432-00
Thermocouple	Omega	GTMQSS-062U-6
Pressure sensor	Omega	PX309-500G5V
Mass flow meter	McMillan	102 Range 8
DAQ software	Wincon for MATLAB	

Table 3.2 Experimental System Parameters

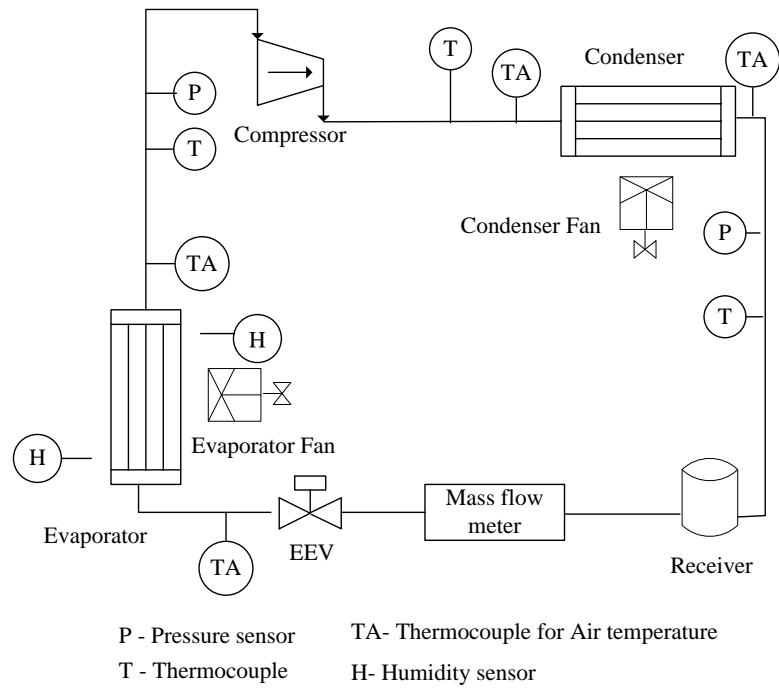| Component	Parameter	Units	Formula used	Calculated Value	Tuned Value	Comment
Evaporator	Mass	$[kg]$	$\rho\pi(R-r)^2 l$	20.64	20	Calculated
	Specific Heat	$[kJkg^{-1}K^{-1}]$	-	-	0.4	Copper
	Surface Area (external)	$[m^2]$	$\pi D l$	1.84	2.723	Tuned
	Surface Area (internal)	$[m^2]$	$\pi d l$	0.5467	2.228	Tuned
	Cross-sectional Area	$[m^2]$	$\pi D^2/4$	7.51e-5	7.51e-5	Calculated
	Length (l)	$[m]$	-	-	60	Measured
	Diameter(D)	$[m]$	-	-	0.0098	Measured
	Inner Diameter (d)	$[m]$	-	-	0.0029	Estimated
Condenser	Mass	$[kg]$	$\rho\pi(R-r)^2 l$	19.72	20	Calculated
	Specific Heat	$[kJkg^{-1}K^{-1}]$	-	-	0.4	Copper
	Surface Area (external)	$[m^2]$	$\pi D l$	3.14	3.955	Tuned
	Surface Area (internal)	$[m^2]$	$\pi d l$	1.4765	3.164	Tuned
	Cross-sectional Area	$[m^2]$	$\pi D^2/4$	7.85e-5	7.85e-5	Calculated
	Length	$[m]$	-	-	100	Measured
	Diameter	$[m]$	-	-	0.01	Measured
	Inner Diameter (d)	$[m]$	-	-	0.0047	Estimated
Compressor	Rate Limit	$[\frac{rpm}{s}]$	-	-	200	Calculated from data

In order to run the experimental system, a Simulink model has been developed to control the various parameters related to the experimental system like evaporator and condenser fan speeds, switching between the different compressor stages etc. The outputs of this model are the various temperature and pressure values recorded from their respective sensors via the DAQ board. These sensor values can be monitored through the Wincon software embedded in the Simulink environment.

The evaporator and condenser fan speeds are controlled through the voltage inputs. The evaporator fan can be controlled over a voltage range of -10V to 10V and condenser fan from 0V to 5V. The system is not equipped with a mass flow sensor to measure the mass flow rates of the air at the condenser and evaporator outlets. In order to approximate the value of air mass flow rate, tests have been conducted on both the heat exchangers to calculate air velocity as a function of the input voltage. Area of cross section and density are used to calculate the mass flow rate of air.

3.1 Evaporator Fan Test

A group of undergraduate students in the laboratory have conducted a series of tests to measure the actual air flow through the evaporator. An anemometer was used to measure air velocity exiting the ducting placed at the top of the air handler unit shown in Figure 3.1(a). The data obtained was fit into a fourth order polynomial computing the outlet air velocity,V, as a function of the input voltage controlling evaporator fan speed, F_v as shown in Equation 3.1. The corresponding curve fit was shown in Figure 3.3.

$$V\left[\frac{m}{s}\right] = 0.004266F_v^4 - 0.08702F_v^3 + 0.4431F_v^2 + 0.8281F_v + 9.616 \qquad 3.1$$
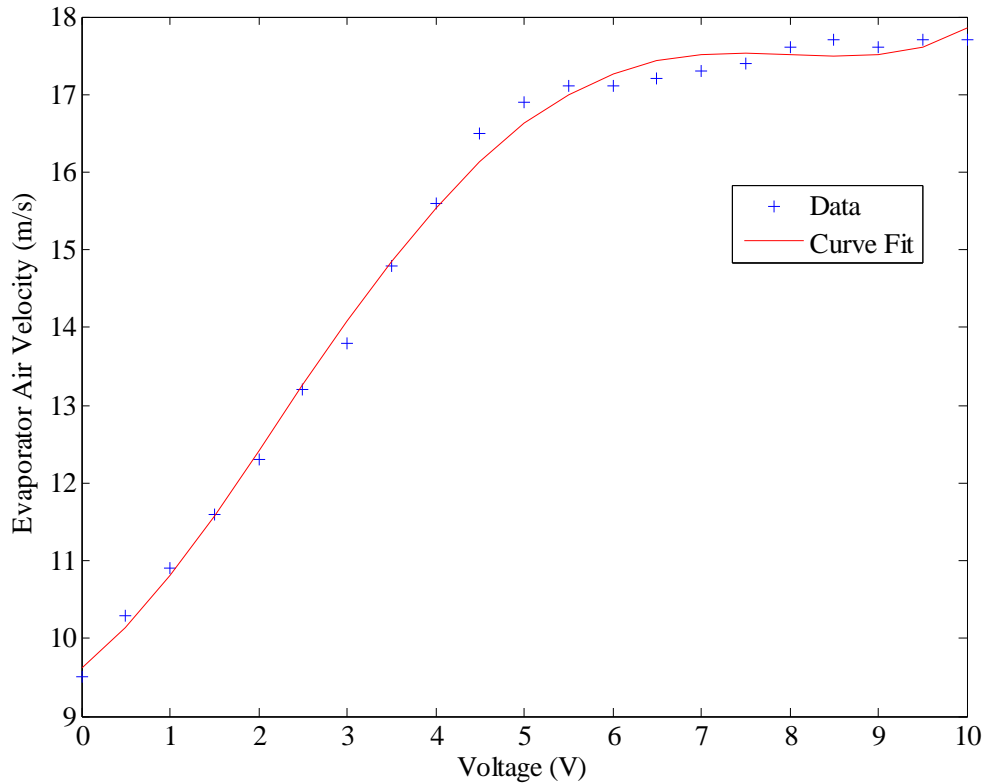
Figure 3.3 Curve Fit for Evaporator Air Velocity vs Fan Voltage

Using Equation 3.1, the volume flow rate of the air leaving the evaporator can be calculated using Equation 3.2, since all the air is exiting through an 8 inch (20.3 cm) round duct.

$$\vartheta = A * V \qquad 3.2$$

We can calculate the density at room temperature using air property tables and the mass flow rate can be calculated using Equation 3.3.

$$\dot{m} = \vartheta * \rho_a \qquad\qquad 3.3$$

3.2 Condenser Fan Test

Similar to the evaporator fan test, an anemometer was used to measure the air velocity exiting the condenser unit. The Equation governing the outlet air velocity, V, and input voltage controlling the condenser fan speed, F_v, is shown in Equation 3.2. The data and the curve fit are plotted as shown in Figure 3.4.

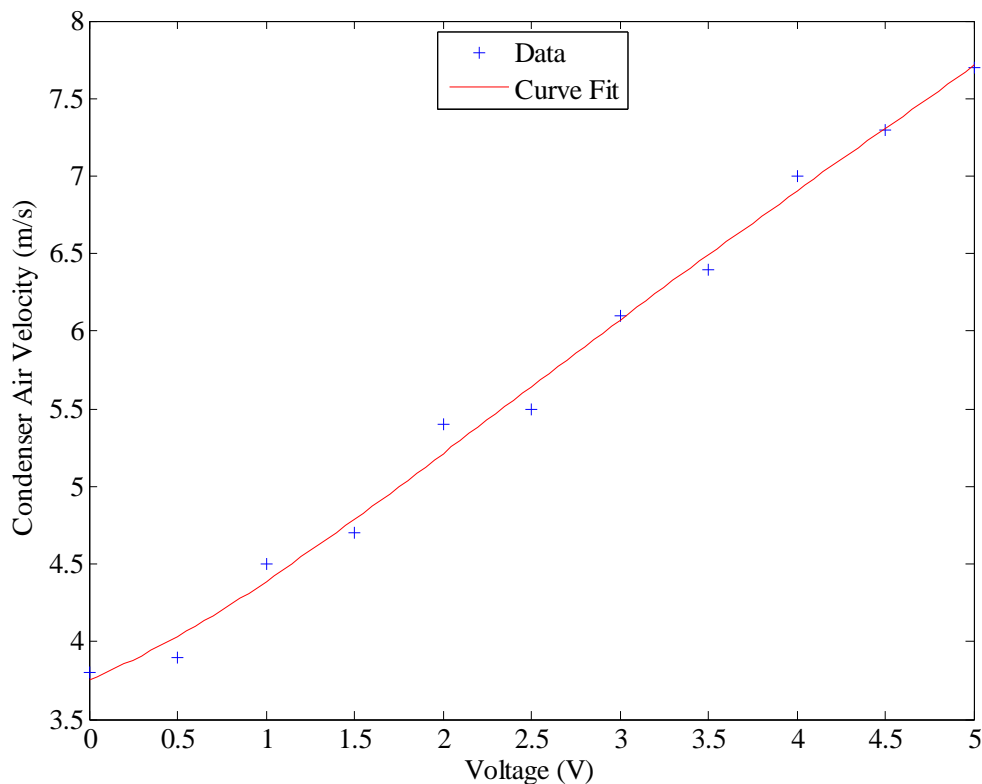$$V\left[\frac{m}{s}\right] = 3.7517 + 0.4763F_v + 0.2015F_v^2 - 0.044F_v^3 + 0.0033F_v^4 \qquad 3.4$$

Figure 3.4 Curve Fit for Condenser Air Velocity vs Fan Voltage

After obtaining the relation for velocity of air as a function of the fan voltage, Equations 3.2 and 3.3 are used to calculate the mass flow rate of air similar to evaporator.

The experimental system was again used to calculate the Reynolds number and j-factor data to measure the external heat transfer coefficient using the Colburn factor heat transfer coefficient. The Reynolds number is calculated using Equation 3.5. The dynamic viscosity is calculated using interpolation from the air property tables.

$$Re = \rho_a * V * D_h / \mu_a \qquad \qquad 3.5$$

The Colburn j-factor is calculated using the Equations 3.6-3.8.

$$Pr = C_p * \mu_a / k_a \qquad \qquad 3.6$$

$$G = \rho_a * V \qquad \qquad 3.7$$

$$j_h = \alpha_o * \frac{Pr^{\frac{2}{3}}}{cp * G} \qquad \qquad 3.8$$

The values of specific heat and thermal conductivity are calculated in the similar manner as the value of dynamic viscosity and the initial estimate of the value of α_o was calculated using the MB model.

The data to create the empirical maps for the compressor and valve is obtained by running the system for various valve positions and pressure values. The curve fits for the values of discharge coefficient, volumetric and adiabatic efficiencies is given in Figures 3.5 through 3.7. The MATLAB code to generate these maps is given in the appendix section.
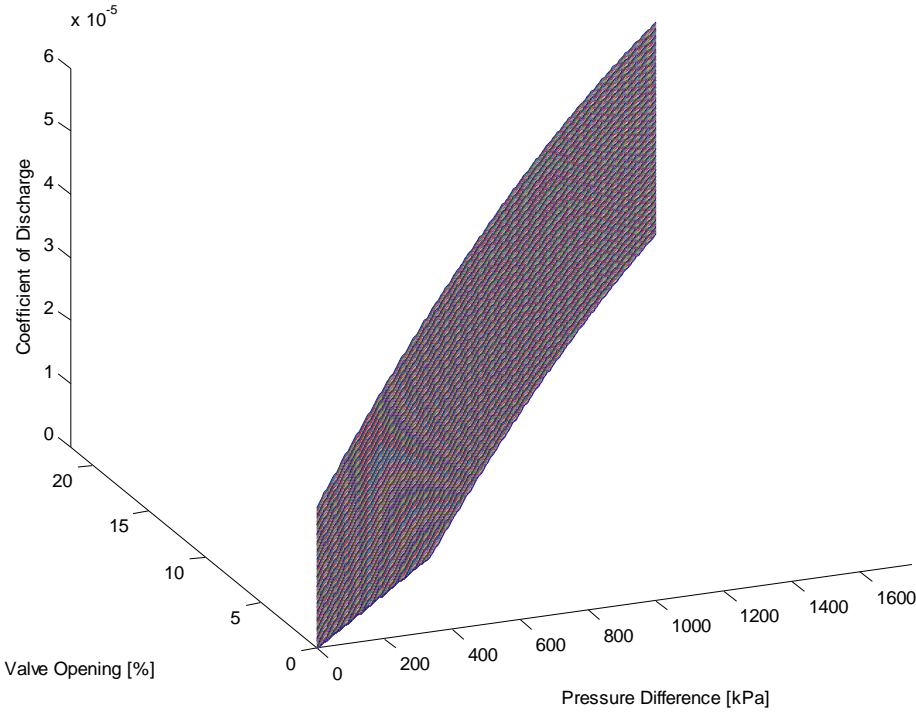
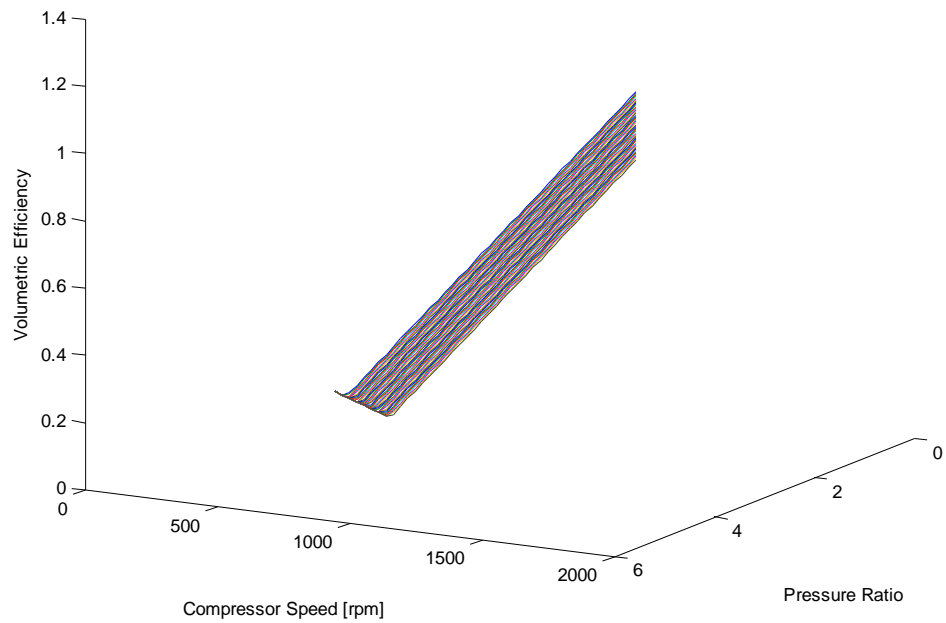**Figure 3.5 Curve Fit of the Discharge Coefficient**

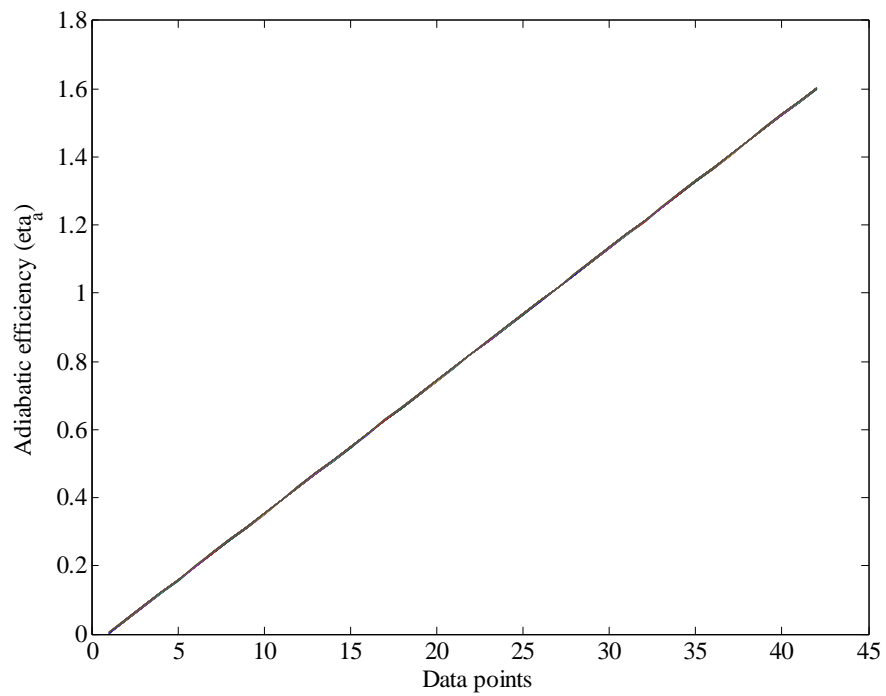**Figure 3.6 Curve Fit of the Volumetric Efficiency**

Figure 3.7 Curve Fit of the Adiabatic Efficiency

4. SIMULATION AND VALIDATION OF FAULTS IN VAPOR COMPRESSION SYSTEMS

Vapor compression cycles are widely used for heating and cooling in industrial, residential, and automotive applications. Due to their widespread use, a great deal of research effort has gone into analyzing the energy efficiency of these cycles. Their failure can be decreased by minimizing the various faults that occur in vapor compression cycles.

Vapor compression system faults are generalized into two classes; hard faults and soft faults. Hard faults are related to the component failures within the system, primarily involving fan or compressor motor failures and valve failures. Soft faults are those that develop slowly over time and include refrigeration loss, heat exchanger fouling, frosting, and internal and external partial blockages in fluid flow.

A number of surveys have been conducted on failures in refrigeration and air-conditioning equipment. The survey performed by Stouppe and Lau in 1989 [12] summarizes 15,760 failures occurred between 1980 and 1987 on various air-conditioning and refrigeration systems. The analysis of the failures suggested that 72% of them were the result of electrical failures with 66% of the total failures occurring in motor windings. In 1998, Breuker and Braun [13] analyzed a company's database which contained over 6000 separate fault cases from 1989 to 1995. They found out that compressor failures accounted for 24% of the total service cost in the database. It was noted that these compressor failures were mainly because of the soft faults. In 2002, Comstock and Braun [14] conducted a survey of common faults in chillers. Similar to

Breuker and Braun, they found that 64% of the repair costs for chillers were the result of compressor and electrical failures. They also concluded that refrigerant leakage was the second most costly fault accounting for 20% of the total service cost. Comstock et.al. noted that 42% of the service calls made to the chillers were due to soft faults. These soft faults also led to premature failure of components, a loss in comfort, or a reduction in efficiency.

Methods based on thermodynamic measurements have been documented by McKellar (1987) [15], Stallard (1989) [16] Wagner and Shoureshi (1992) [17] Grimmelius et al. (1995) [18], Stylianou and Nikanpour (1996) [19], and Rossi and Braun (1997) [20]. The faults considered include compressor valve leakage, heat exchanger fan failures, evaporator frosting, condenser fouling, evaporator air filter fouling, liquid line restriction and refrigerant leakage. Typically temperature and pressure measurements have been considered because of their relatively low cost. Keir and Alleyne [21] have developed simulation models (using moving boundary approach for the heat exchangers) for the fault conditions of evaporator frosting, refrigerant and valve leakages. The dynamic impact of these faults on the vapor compression systems have been discussed by providing simulation results with respect to air-side faults, refrigerant leakage and frost formation. They concluded that a larger static change in system operating condition will help us to detect a slow forming air-side fault while a simultaneous change in the static and dynamic characteristics can be used to detect a rapid forming air-side fault.

Majority of the faults that occur in vapor compression cycles are related to electrical failure in compressors, a result of being overworked due to soft faults. These soft faults force the system to run at higher pressure differential resulting in excess load on the compressor which leads to decrease in the efficiency of the windings and hence the system efficiency. This thesis mainly focuses on soft faults which are much more difficult to detect and may result in catastrophic component failures. Typical soft faults which form a majority of failures in vapor compression cycles are:

- Evaporator and Condenser fouling

- Evaporator frosting

- Compressor valve leakage

- Blockage of electronic expansion valve

Simulation of the faults mentioned above can be achieved by varying the parameters whose values change when the actual fault occurs. We call these parameters as 'model variables'. The parameters which are affected with the change in model variables are categorized as 'output variables'. The transients resulting from the simulations are classified into two modes:

- **Sudden change in model variables**

  In this mode, a step input is given to each of the model variables corresponding to that fault at a particular time interval and changes are observed in the output variables. The step input replicates the change in the model variables when fault occurs in the system.

- **Model sensitivity to parameter variations**

  In this mode, the input parameters like speed of the compressor and/or valve command signal are given step inputs and output variables are calculated for two different constant values of the model variables. This analysis is performed because the data received by giving a step input to model variables might not be always conclusive in predicting a particular fault, especially when considering certain faults such as Evaporator Frosting that develop over a period of time. In such a case the concept of giving step input is of very little significance.

The experimental system described in Section 3 has been used to perform the validation of the simulation results. Owing to the complexity of introducing the faults artificially into the experimental system, we have decided to limit ourselves to validating four out of the seven faults simulated namely, External Evaporator Fouling, External Condenser Fouling, Blockage of Electronic Expansion Valve and Compressor Valve Leakage.

The rest of this section has been organized as follows: Subsection 4.1 deals with description, simulation results and validation results related to heat exchanger fouling. Subsection 4.2 focuses on the various parameters and simulation results related to evaporator frosting. Simulation and validation results related to compressor valve leakage and blockage of electronic expansion valve make up Subsections 4.3 and 4.4 respectively.

4.1 Heat Exchanger Fouling

Evaporator and condenser fouling can be known together as heat exchanger fouling. Heat exchanger fouling is defined as build up of a thermally insulating material on a heat transfer surface. It can be divided into External and Internal.

4.1.1 Previous Work on Heat Exchanger Fouling

Epstein [22] presented a general discussion of fouling modes in heat exchangers. This paper talks about categorizing the fouling into six methods depending on the method of deposit formation on the surface of the heat exchanger namely scaling, particulate fouling, chemical reaction fouling, corrosion fouling, biofouling, and freezing fouling. A study of fouling specific to HVAC systems was discussed by Siegel and Nararoff [23]. This paper mainly talks about the external fouling in the heat exchanger. When the external fluid is air, they identified particulate fouling as the primary mode for fouling in HVAC systems. Wilhelmsson, B. [24] talked about the effect of the type of heat exchanger on the fouling. Upon discussion of the various factors like the geometry, cost etc. he concluded that Spiral Heat Exchangers (SHE) will be the best overall choice for heat exchanger duties when compared to the traditional shell & tube heat exchangers.

4.1.2 Thermodynamic Impact of Heat Exchanger Fouling

- **External fouling** of heat exchanger will impact the vapor compression system in two different ways. The thermal resistance between the air and the refrigerant increases with the buildup of an insulating material on the surface of the heat

exchanger. Increase in size of this layer on a conventional tube heat exchanger causes a reduction in the free flow area through the fins which in turn decreases the mass flow rate of the air passing over the heat exchanger. Reduction in the free flow area also causes an increase in the pressure differential [25] i.e. an increase in the condenser pressure and a decrease in the evaporator pressure.

4.1.3 Simulation Results for External Evaporator Fouling

Model variables: Mass flow rate of the air [kg/s]

Output variables: Pressure at the evaporator [kPa]; Superheat temperature [℃]

Simulation results:

- **Sudden change in model variables**

  This can be visualized as a system wherein the evaporator has been blocked suddenly by leaves or debris. The step input is given to the mass flow rate of air and changes in the output variables are observed. All the output variables-evaporator pressure and superheat temperature decrease when step input is given, as shown in Figure 4.1. This is in sync with the explanation provided above.

- **Model sensitivity to parameter variations**

  In this the step input is given to the valve opening and outputs are calculated for two constants values of mass flow rate of the air. This analysis of the variation in the output variables for two different constant values of the mass flow rate of air is useful when the fouling develops over a period of time. The concerned plots are shown in Figure 4.2.
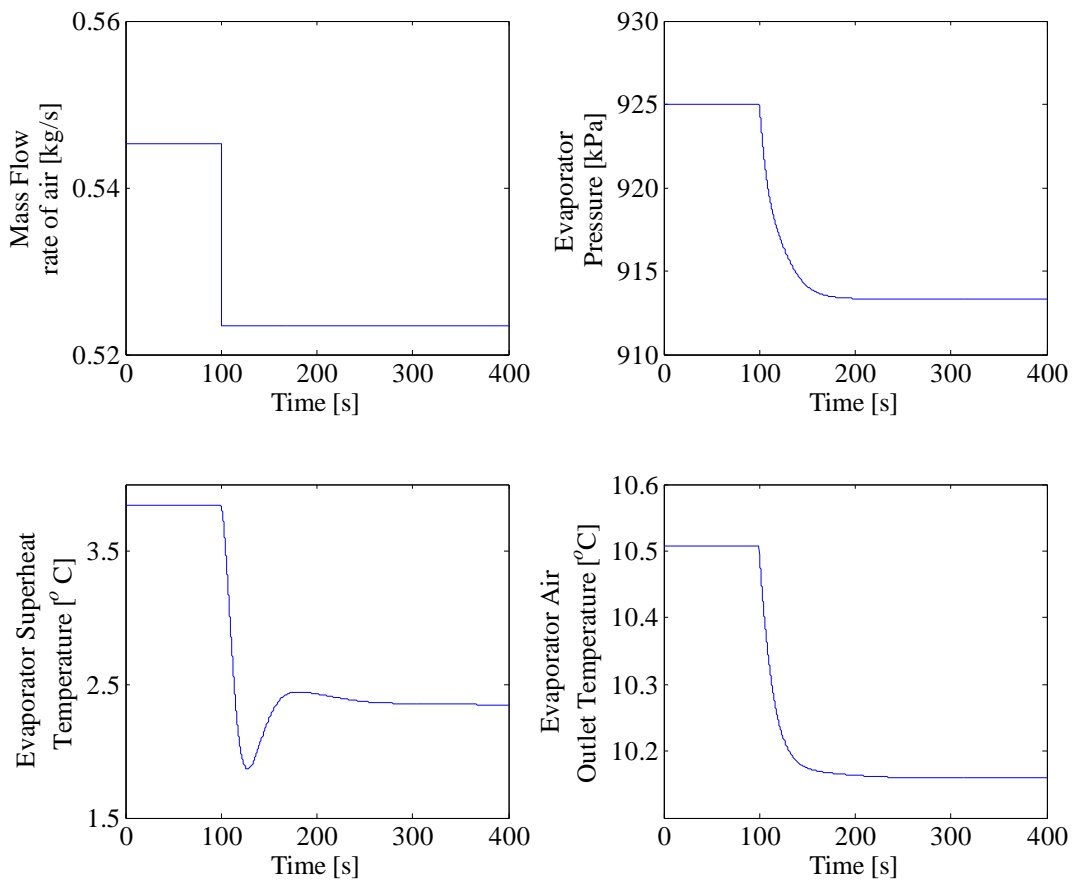
Figure 4.1 Simulation of External Evaporator Fouling for Sudden Change in Model Variables

4.1.4 Validation Results for External Evaporator Fouling

In general, previous studies have either used a reduction in the mass flow rate of the external fluid or the introduction of a blockage into the external fluid flow path to assess the impact of fouling on a vapor compression system [21, 26]. In this case, artificial evaporator fouling fault was introduced in the experimental system by reducing the voltage corresponding to the evaporator fan speed which is equivalent to reduction of the
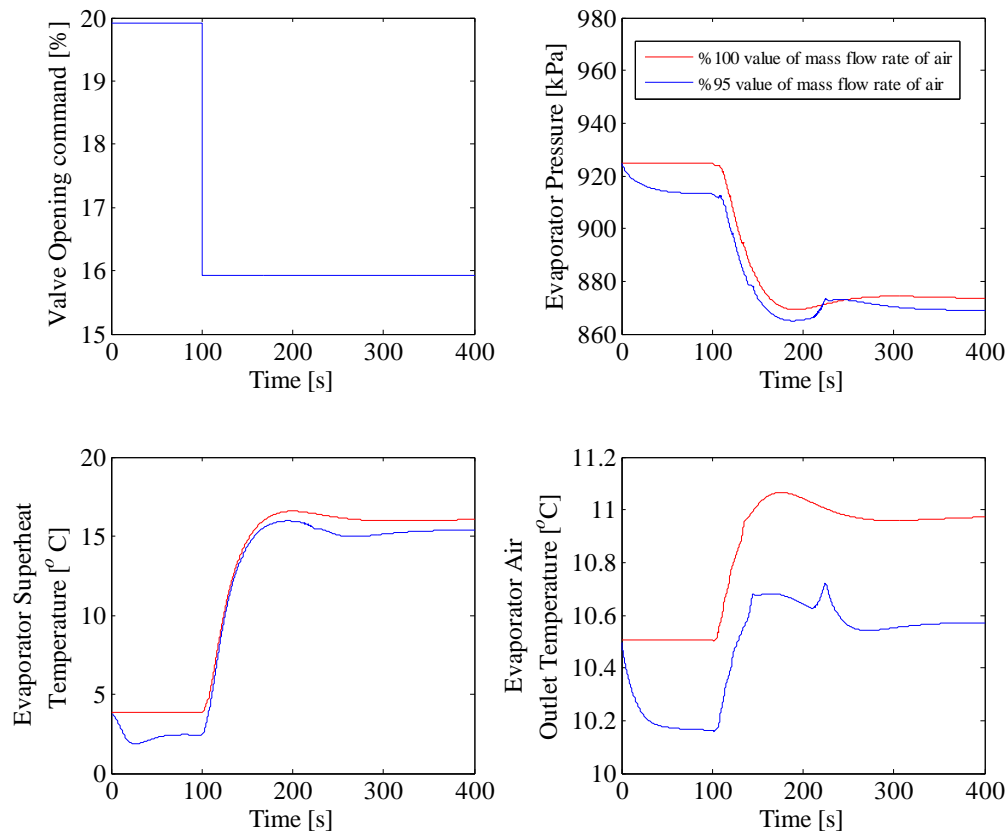
Figure 4.2: Simulation of External Evaporator Fouling for Model Sensitivity in Parameter Variations

mass flow rate of the air over the evaporator. The validation results for this case are shown in Figure 4.3. The plot consists of experimental results for step change in evaporator far speed as well as partially blocking the evaporator intake with a piece of cardboard. As seen from Figure 4.3, the magnitude and transient of evaporator superheat temperature are similar for both the experimental scenarios while the steady state pressure value is different as they are carried out on two different days with different experimental conditions. However, the nature of transient for pressure and temperature values after the introduction of fault in both cases is similar. Blocking the evaporator

does not provide a 100% effective seal and hence step change in evaporator fan speed is considered for the purpose of validation.
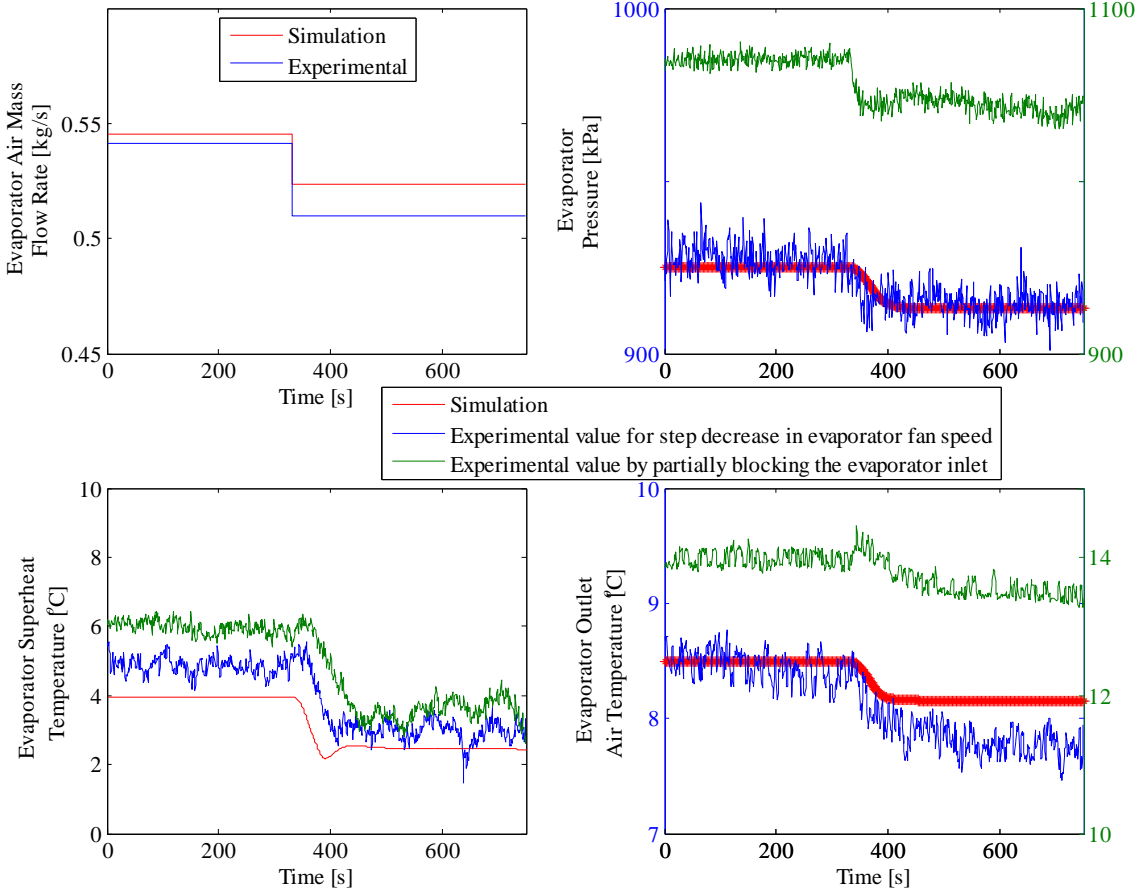
Figure 4.3 Validation of External Evaporator Fouling

4.1.5 Simulation Results for External Condenser Fouling

Model variables: Mass flow rate of the air [kg/s]

Output variables: Pressure at the condenser [kPa]; Temperature of refrigerant at the condenser outlet [ºC]

Simulation results:

- **Sudden change in model variables**

  This can be visualized as a system wherein the condenser has been blocked suddenly by leaves or debris. The step input is given to the mass flow rate of the air at the time instant of 100 seconds and the changes in the output variables are observed. All the output variables- condenser pressure and temperature of refrigerant at the condenser outlet increase when the step input is given. As seen from Figure 4.4, the condenser pressure and outlet refrigerant increase with the step change in mass flow rate of air. This is in sync with the explanation provided above.

- **Model sensitivity to parameter variations**

  In this the step input is given to the valve input command and outputs are calculated for two constants values of mass flow rate of the air. This analysis of the variation in the output variables for two different constant values of the mass flow rate of air is useful when the fouling develops over a period of time. The concerned plots are shown in Figure 4.5.
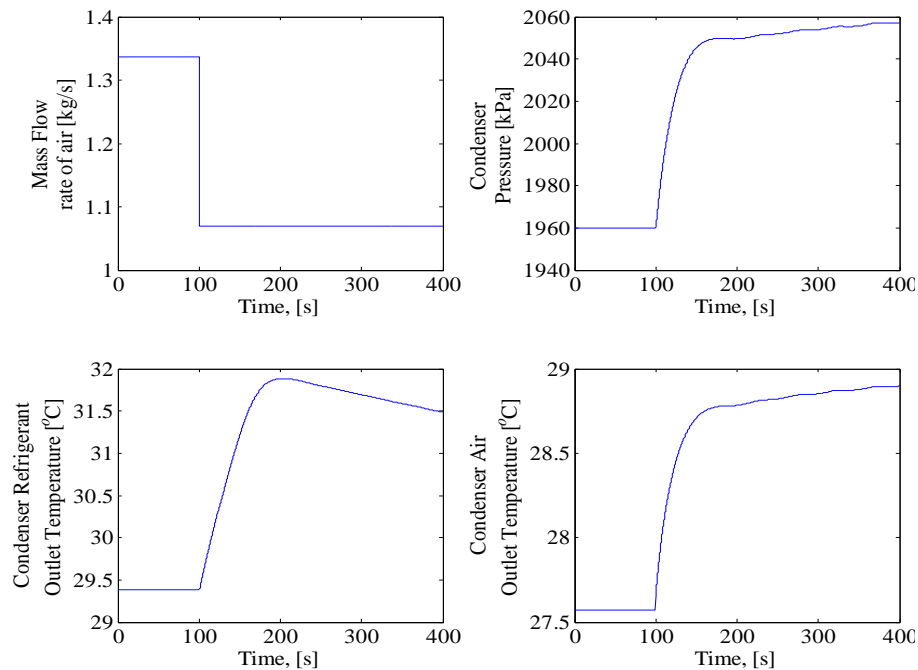
Figure 4.4 Simulation of External Condenser Fouling for Sudden Change in Model Variables

4.1.6 Validation Results for External Condenser Fouling

Condenser fouling is equivalent to having a smaller condenser and leads to higher condensing temperatures and pressures than for the normal (no fault) case. Similar to evaporator fouling, artificial condenser fouling fault was introduced in the experimental system by reducing the voltage corresponding to the condenser fan speed which is equivalent to reduction of the mass flow rate of the air over the condenser. The validation results for this case are shown in Figure 4.6. The plot consists of experimental results for step change in condenser far speed as well as partial blockage of condenser with a piece of cardboard. The initial steady state conditions for both the experiments are different as they are carried out at different experimental conditions.
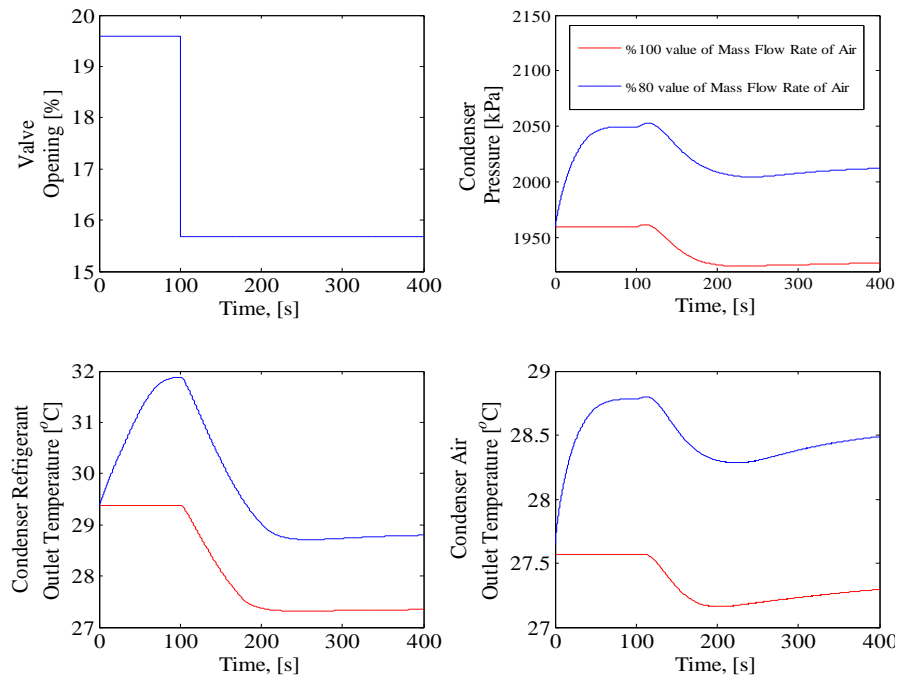
Figure 4.5 Simulation of External Condenser Fouling for Model Sensitivity in Parameter Variations

As can be seen from Figure 4.6, the change in the pressure and temperature for experimental condition of physical blocking is slightly less than the change arising due to step change in evaporator fan speed. This might be due to the fact that physically blocking the condenser does not provide a 100% effective seal and some amount of air can always escape from the sides. But the nature of the transient for the two conditions is the same as seen in Figure 4.6. Due to this inconsistency with physically blocking the condenser, validation with step change in condenser fan speed is considered a better result.

4.1.7 Summary of the Results for External Heat Exchanger Fouling

Figure 4.1 shows the results for 5% step decrease in the mass flow rate of the air for evaporator fouling and Figure 4.5 shows the results for 20% step decrease in the mass flow rate of the air for condenser fouling. From the two Figures, we can see that even though there is a greater step decrease for the mass flow rate of the air related to condenser fouling, the pressure and refrigerant changes are more pronounced for evaporator fouling than for condenser fouling. This shows that the condenser fouling is harder to detect than evaporator fouling. This result is in sync with the analysis made by Keir and Alleyne [21] where they prove the similar result.
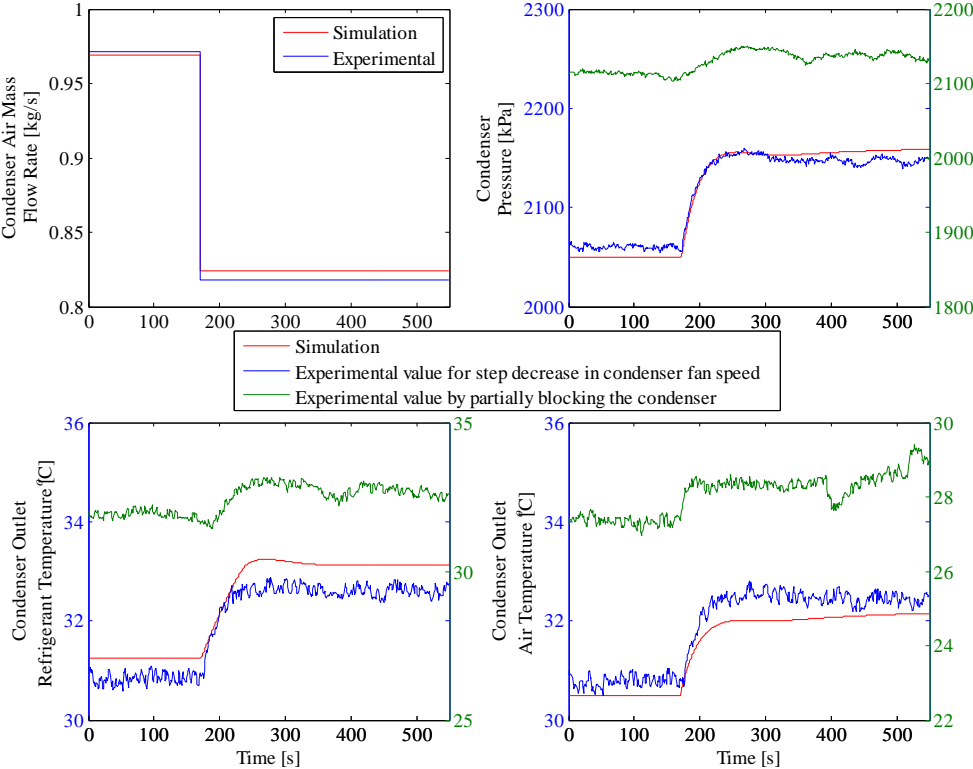

Figure 4.6 Validation of External Condenser Fouling

- **Internal Fouling** in a heat exchanger occurs when a fluid goes through the heat exchanger, and the impurities in the fluid precipitate onto the surface of the tubes. This results in reduction in internal cross-section area for the heat to be transferred and causes an increase in the resistance to heat transfer across the heat exchanger. This is because the thermal conductivity of the fouling layer is low. This reduces the overall heat transfer coefficient and efficiency of the heat exchanger. This in turn, can lead to an increase in pumping and maintenance costs.

4.1.8 Simulation Results for Internal Evaporator Fouling

Model variables: Heat transfer coefficient between the tube wall of the evaporator and refrigerant [W/ (m°C)]

Output variables: Pressure at the evaporator [kPa]; Evaporator Refrigerant Outlet Temperature [°C]

Simulation results:

- **Sudden change in model variables**

  Here, one extra disturbance input is considered for the evaporator model. The steady state operating condition value of this variable is set to one and is multiplied with the already existing values of the internal heat transfer coefficient. In order to introduce a step change in the value of the internal heat transfer coefficient, it is sufficient to bring about a step change in this disturbance input. This will bring about a proportional change in the model variables.

Considering the above argument, step change is given to the disturbance input and changes in output variables are recorded. The result is shown in Figure 4.7.

- **Model sensitivity to parameter variations**

  Step input is given to valve opening command and output variables are plotted for two different constant values of internal heat transfer coefficient between air and evaporator walls. The result is shown in Figure 4.8.
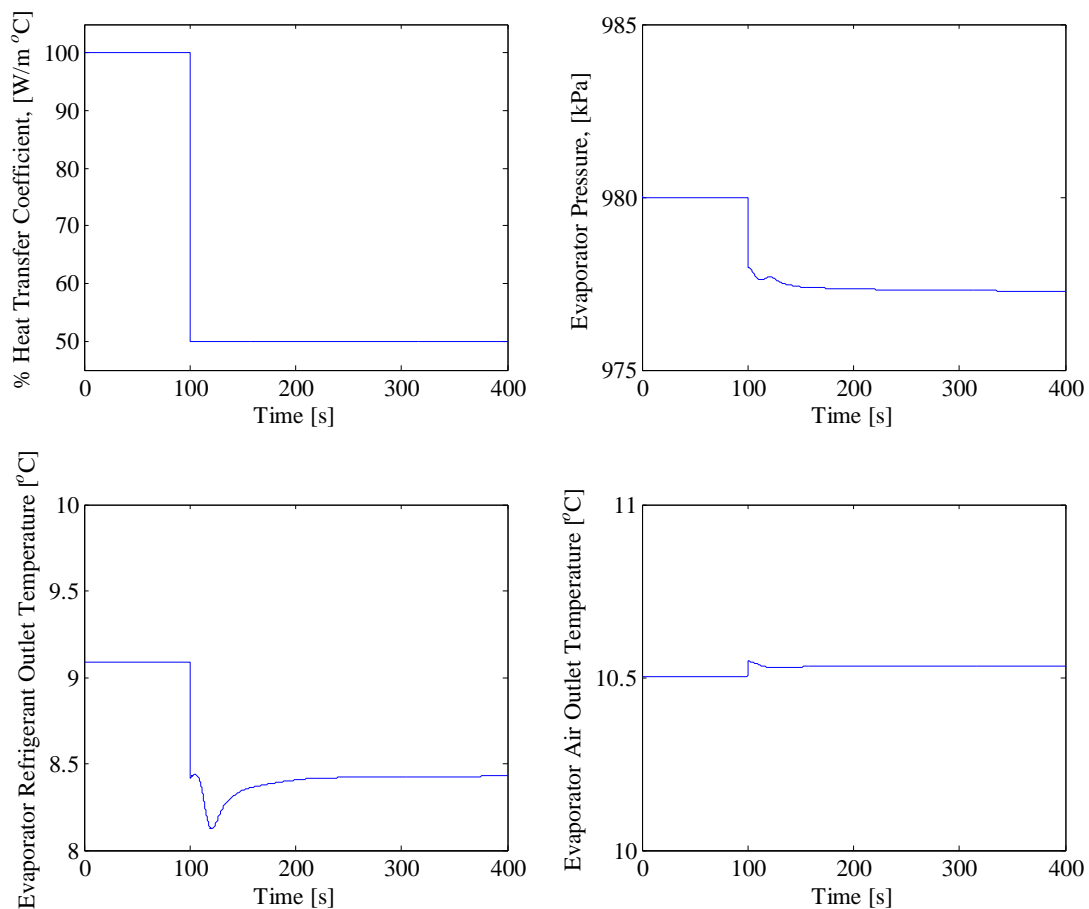
Figure 4.7 Simulation of Internal Evaporator Fouling for Sudden Change in Model Variables
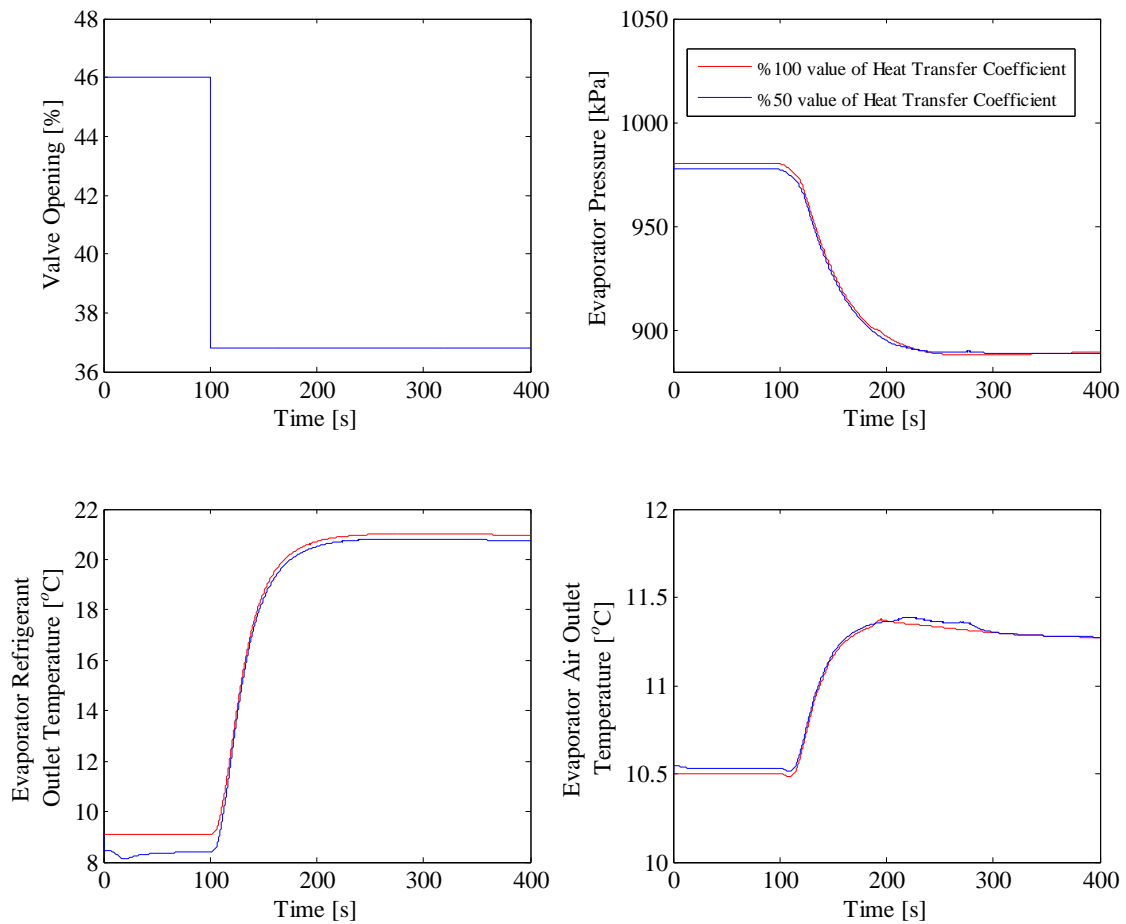
Figure 4.8 Simulation of Internal Evaporator Fouling for Model Sensitivity to Parameter Changes

4.1.9 Simulation Results for Internal Condenser Fouling

Model variables: Heat transfer coefficient between the tube wall of the condenser and refrigerant [W/ (m.C)]

Output variables: Pressure at the condenser [kPa]; Temperature of refrigerant at the condenser outlet [ºC]

Simulation Results:

- **Sudden change in model variables**

  Here, one extra disturbance input is considered for the condenser model. The steady state operating condition value of this variable is set to one and is multiplied with the already existing values of the internal heat transfer coefficient. In order to introduce a step change in the value of the internal heat transfer coefficient, it is sufficient to bring about a step change in this disturbance input. This step change in the model variables brings about a change in the output variables as shown in the Figure 4.9.

- **Model sensitivity to parameter variations**

  Step input is given to valve command input and output variables are plotted for two different constant values of internal heat transfer coefficient between air and condenser walls as shown in Figure 4.10.

*4.2 Evaporator Frosting*

Frosting of the evaporator occurs when the temperature on the surface of the evaporator is below the dew point of air and below the freezing point of water.

4.2.1 Previous Work on Evaporator Frosting

Thybo et. al. [27] showed that the reduction in mass flow rate due to evaporator frosting was the dominant effect on supermarket refrigerated display cabinets. They proved experimentally that the temperature drop across the evaporator increased with the

formation of the frost, indicating that the reduction in mass flow rate dominated the effect of reduction in heat transfer coefficient. In 2004, Seker et. al. provided simulation results by introducing the pressure drop correlation developed by Kays and London [28] to the frost model developed by Kondepudi and O'Neal [29]. Finite control volume model was used and a variety of correlations were applied related to the heat exchanger geometry to capture the heat transfer characteristics. Experimental validation of evaporator frosting was presented by Yao et. al. [30] using a finite control heat exchanger model. J-factor method was incorporated to develop the external flow and heat transfer characteristics.
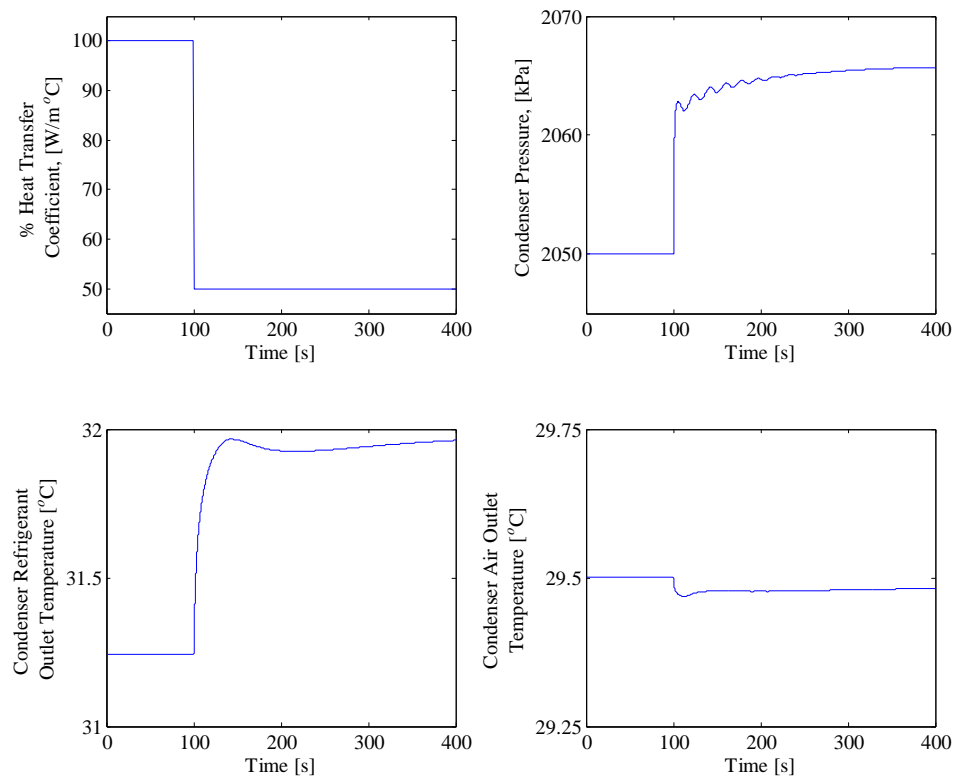
Figure 4.9 Simulation of Internal Condenser Fouling for Sudden Change in Model Variables
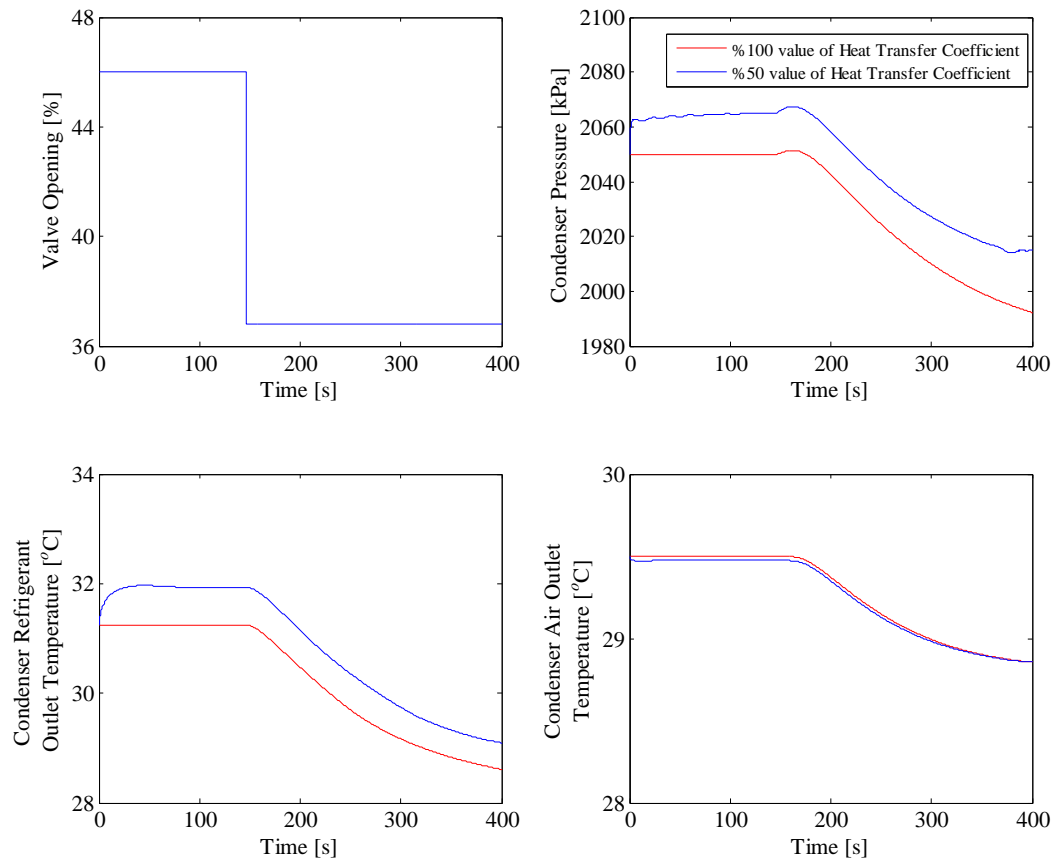
Figure 4.10 Simulation of Internal Condenser Fouling for Model Sensitivity to Parameter Changes

4.2.2 Thermodynamic Impact of Evaporator Frosting

As the amount of frost increases, initially the heat transfer rate between the air and walls also increases because of the increase in surface area [16]. But as the amount of frost continues to increase, the evaporator experiences an increase in pressure drop and decrease in heat transfer rate. Also since the area of cross-section decreases, there will be a reduction in the mass flow rate of the air flowing through the evaporator thus decreasing the temperature of the air at the evaporator outlet. This lowering of

evaporator temperature may create mechanical problems in the system such as liquid refrigerant flood back to the compressor.

4.2.3 Simulation Results for Evaporator Frosting

Model variables: mass flow rate of air [kg/s]; Heat transfer coefficient between the tube wall of the evaporator and air [W/ (m°C)]

Output variables: Pressure at the evaporator [kPa]; Superheat temperature [°C]

Simulation results:

In this case, we are assuming that the evaporator frosting develops over a period of time because of which we are only considering the model sensitivity to parameter changes.

- **Model sensitivity to parameter variations**

  Step input is given to speed of the compressor and output variables are plotted for two different constant values of mass flow rate of air and heat transfer coefficient between air and evaporator walls. Figure 4.11 shows the relevant plots. The results presented here agree with the explanation provided in the thermodynamic analysis Subsection above.
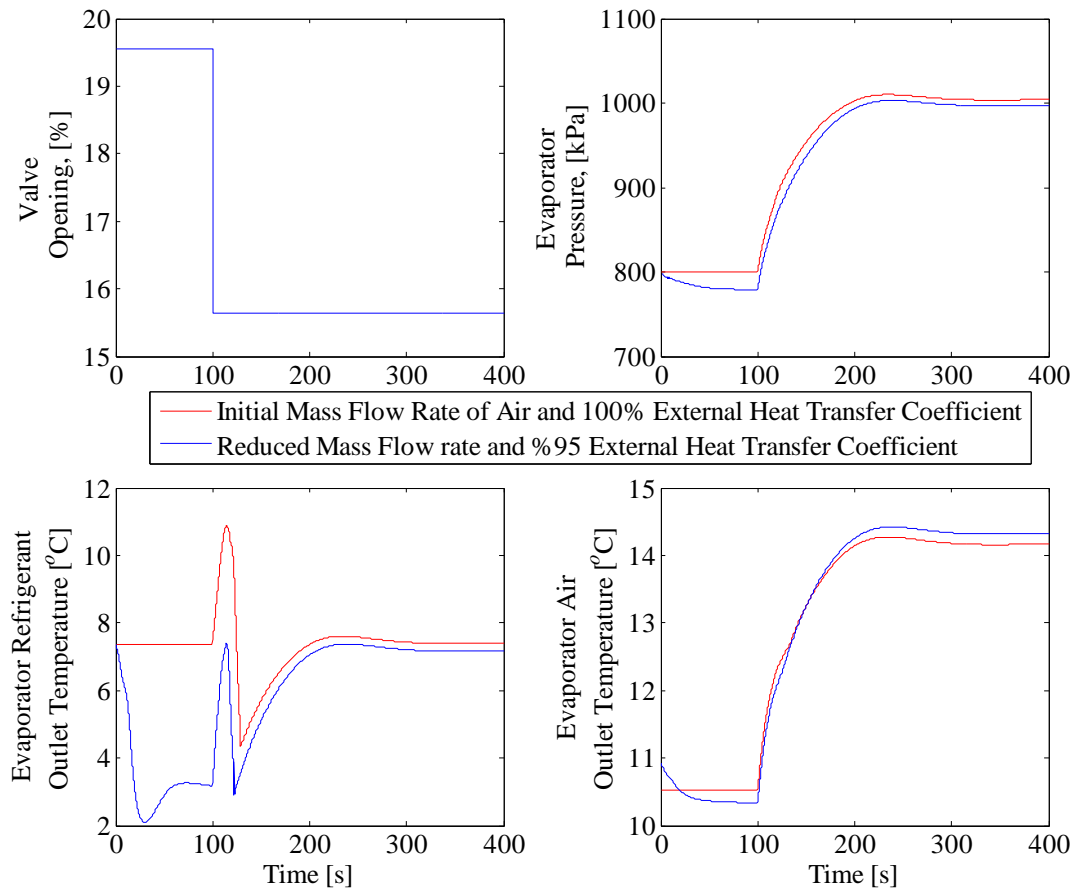
Figure 4.11 Simulation of Evaporator Frosting for Model Sensitivity to Parameter Changes

4.3 Compressor Valve Leakage

Compressor valve leakage is meant to include any fault within the compressor that leads to a loss in volumetric efficiency and refrigerant flow rate. It is one cause of a reduction in the capacity of a compressor. It is typically caused by slugs of liquid refrigerant which damage the suction valve in the compressor, causing it to lose an effective seal. When this happens, some of the high pressure refrigerant in the compression cylinder leaks back into the suction line across the suction valve.

4.3.1 Previous Work on Compressor Valve Leakage

Kim et. al. [25] and Breuker and Braun [13] simulated the compressor valve leakage by opening a bypass valve that allows the refrigerant to flow back from the discharge line into the suction line. The percentage reduction in the net volumetric efficiency was calculated using known compressor specifications.

4.3.2 Thermodynamic Impact of Compressor Valve Leakage

Leaking valves are the most common faults in compressors. At high-pressure stages, both inlet and discharge valves are exposed to high-speed flow, high temperature and high vibro-impacts. This results in non-uniform wear of the sealing surfaces between the valve plate and its seat, eventually causing leakage. Breuker and Braun [13] have shown that this leak causes the superheat temperature to decrease which also causes a reduction in the volumetric efficiency of the compressor.

4.3.3 Simulation Results for Compressor Valve Leakage

Model variables: Volumetric efficiency

Output variables: Pressure at the evaporator [kPa]; Evaporator Superheat temperature [ºC]; Pressure at the condenser [kPa]

Simulation results:

- **Sudden change in model parameters**

    To achieve a step change in the volumetric efficiency, a disturbance input is introduced into the compressor model. The default value of this disturbance input

is one and is multiplied with the already existing value of volumetric efficiency. Any step input given to this new input will automatically result in a step change in the volumetric efficiency. The relevant plots are shown in Figure 4.12 the results of which are similar to the explanation provided in the thermodynamics Subsection above.

- **Model sensitivity to parameter variations**

Step input is given to valve input command, keeping the speed of the compressor constant, and output variables are plotted for two different constant values of volumetric efficiency. The concerned plots for this case are shown in Figure 4.13.
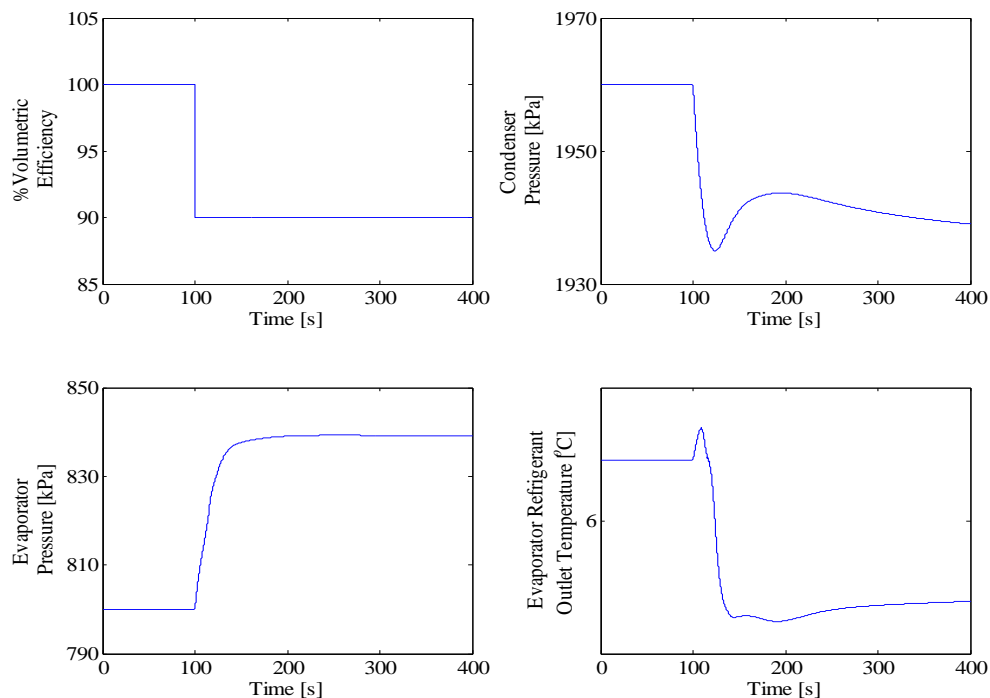
Figure 4.12 Simulation Compressor Valve Leakage for Sudden Change in Model Variables
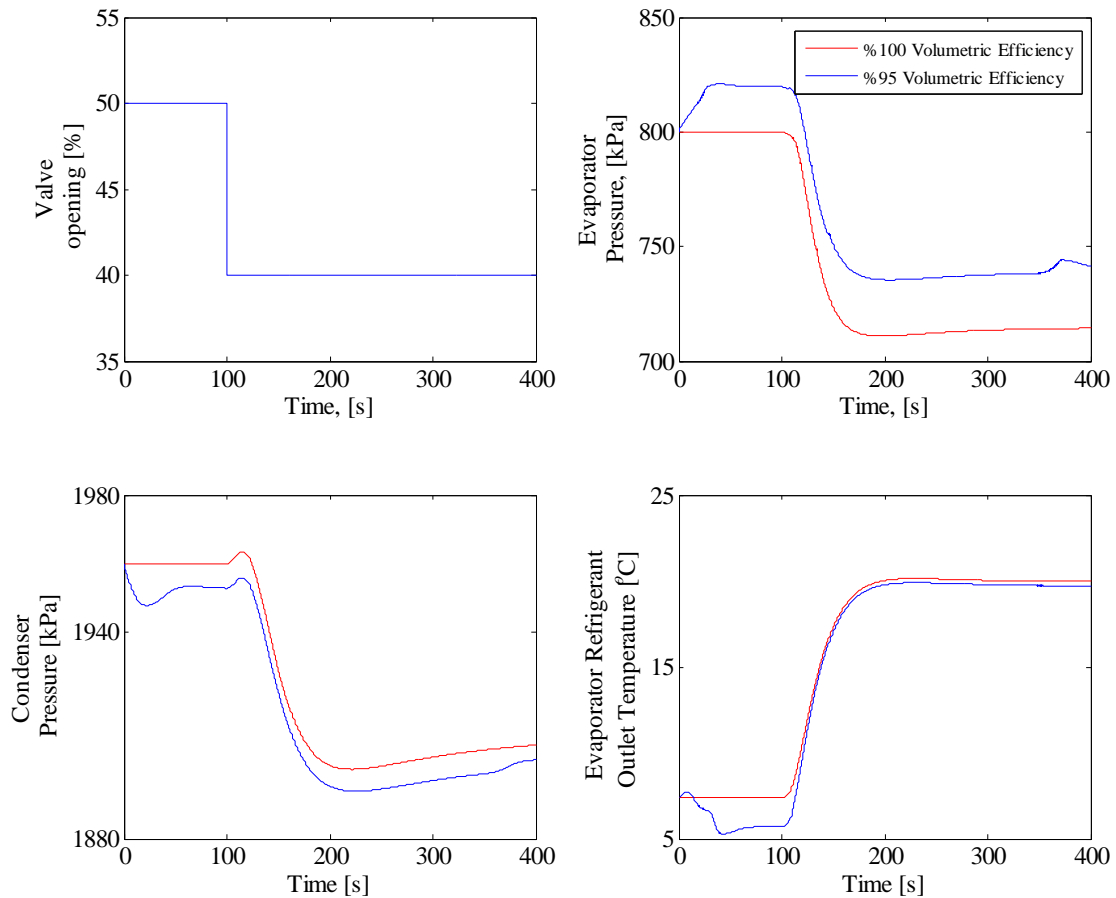
Figure 4.13 Simulation of Compressor Valve Leakage for Model Sensitivity to Parameter Variations

4.3.4 Validation Results for Compressor Valve Leakage

The existing set-up had to be modified to introduce this fault artificially in the experimental system. A bypass valve was installed, with the help of Matt Elliot, between the suction and discharge lines and is shown in Figure 4.14. To replicate the fault, this bypass valve was opened which allows the refrigerant to flow back from the discharge line into the suction line. The validation results for this fault are shown in Figure 4.15.

Figure 4.14 Bypass Valve Installed on the TRANE System
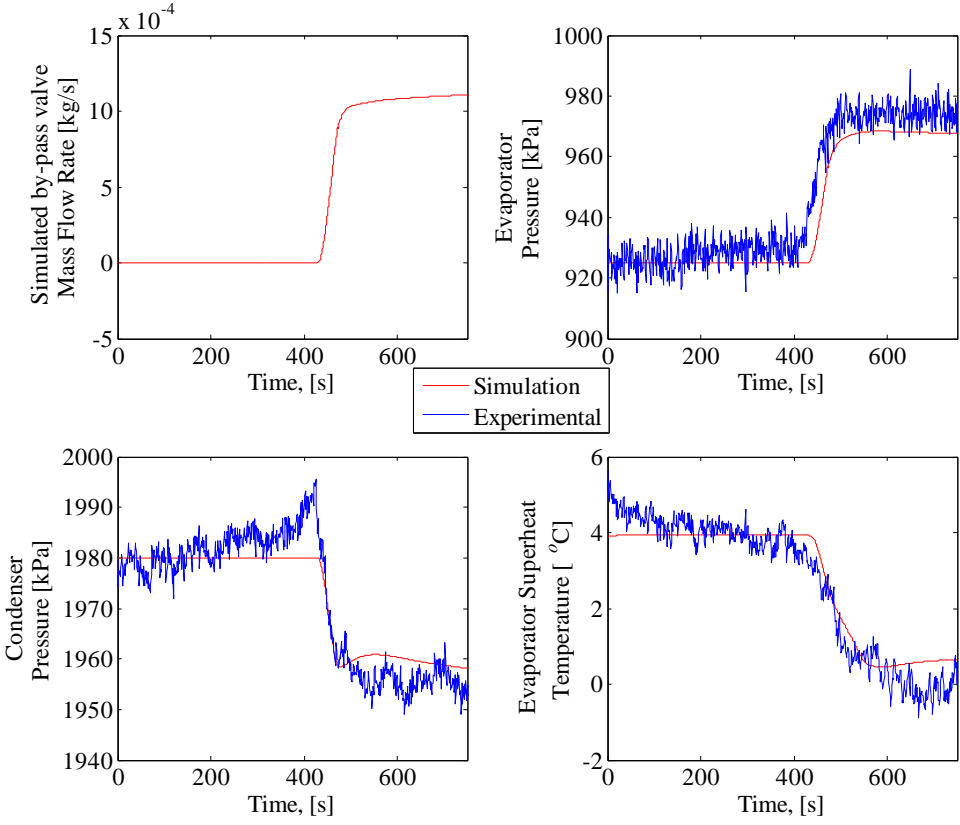
Figure 4.15 Validation of Compressor Valve Leakage

4.4 Blockage of Electronic Expansion Valve

Electronic Expansion Valve is a relatively modern type of expansion valve used in AC&R systems. It consists of a needle valve controlled by a stepper motor. Thus the pressure drop and the mass flow rate through the valve can be controlled by controlling the area of opening of the valve which in-turn is regulated by the stepper motor.

4.4.1 Thermodynamic Impact of Blockage of Electronic Expansion Valve

When there is a blockage in the expansion valve, the refrigerant flow is not regulated. With an insufficient amount of refrigerant, the coil is starved and operates at a reduced capacity. This results in the refrigerant being drawn intermittently into the compressor in slugs thus damaging the compressor.

4.4.2 Simulation Results for Blockage of Electronic Expansion Valve

Model variables: Valve Command (percentage of valve opening)

Output variables: Pressure at the evaporator [kPa]; Evaporator Superheat temperature [ºC];

Simulation results:

In this case, we are assuming that the blockage of the valve is instantaneous and cannot be developed over a period of time.

- **Sudden change in model parameters**

  This can be visualized as a system wherein the valve has been partially blocked impeding the mass flow rate of the refrigerant. In this simulation, a step input is

given to the valve command signal, replicating the condition when the valve is blocked. The following plots (Figure 4.16) show the changes in the output variables for the step input change:
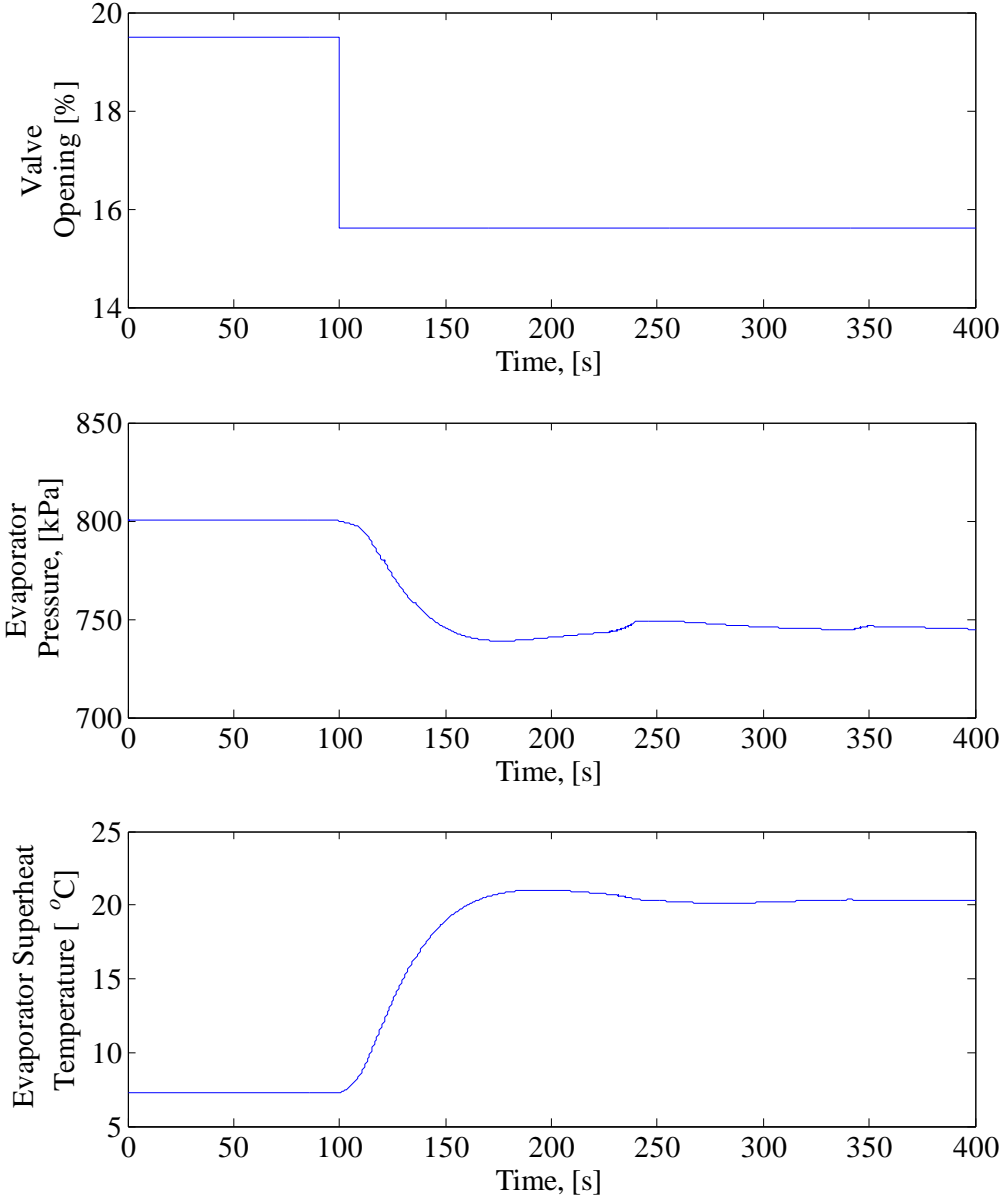
Figure 4.16 Simulation of Blockage of Electronic Expansion Valve for Sudden Change in Model Variables

4.4.3 Validation of Blockage of Electronic Expansion Valve

Electronic expansion valve blockage fault was introduced in the experimental system by reducing the amount of valve opening which is achieved by decreasing the value of the command signal corresponding to the valve input. The validation results for this case are shown in Figure 4.17.
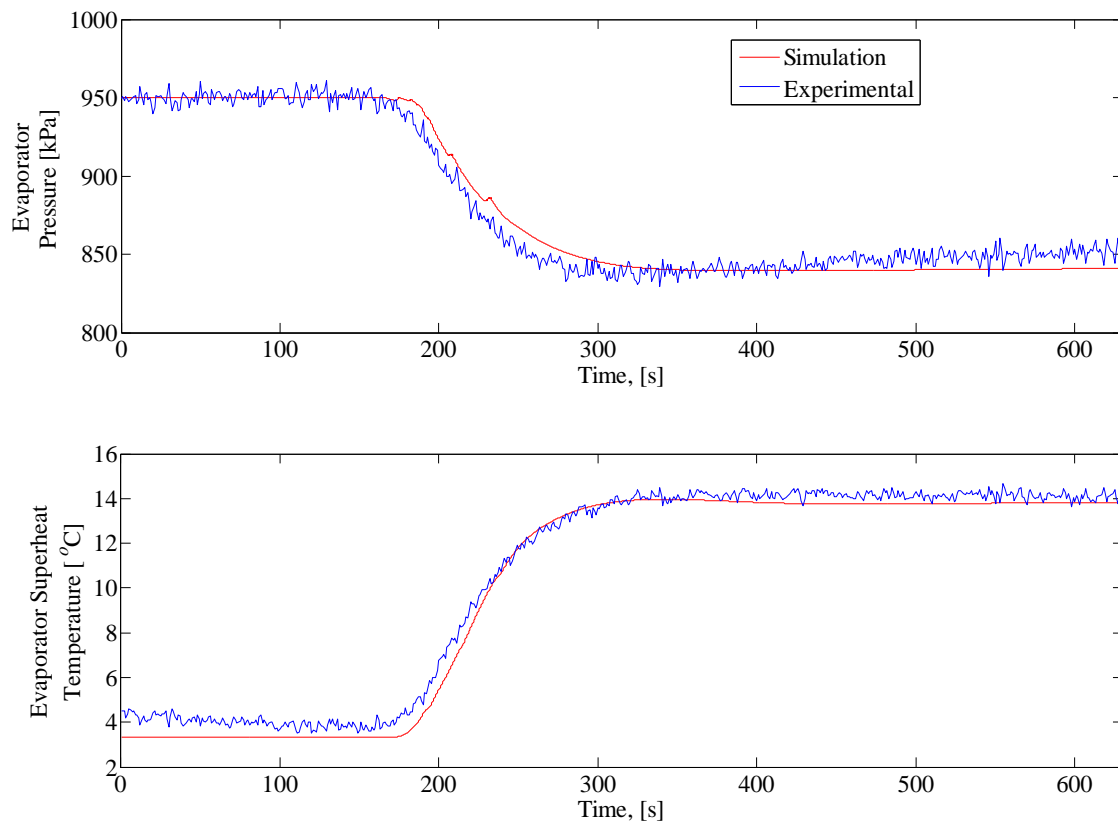
Figure 4.17 Validation of Blockage of Electronic Expansion Valve

5. SIMULATION AND VALIDATION OF START-UP/SHUTDOWN TRANSIENTS IN VAPOR COMPRESSION SYSTEMS

The classification of the complete operation cycle of a vapor compression system is based on two major time-regimes, namely transient and steady state. As the name suggests, the latter part is concerned with the system input/output parameters that are constant over time; transient operation is then, by default, the non-steady state [31]. Typically, this is the case when the system is started-up and is approaching steady state, or when it is shutdown from a steady state. These are, in general, termed as the start-up and shutdown transients and account for the greater part of cyclic losses occurring in air conditioning systems. These occur mainly due to changes in space loads and outdoor air loads, control loop operation etc. The dynamics of the refrigerant are regarded as the primary cause for the delay in reaching the steady-state conditions upon start-up [32]. Judge et al. [33] stated that on-off cycling of the system results in degradation of the coefficient of performance (COP) of the system to values below 75% of the steady state values. All these factors emphasize the importance of the study of transient characteristics from the point of actual energy efficiency of the systems.

The transient characteristics of the air-conditioning systems have been reported by many researchers, based on the experimental studies. Murphy and Goldschmidt have carried out significant analysis on the various conditions of start-up and shutdown. Their paper [34] on the evaluation of the efficiency of a residential unit under cyclic behavior concludes that the transient losses due to cycling differ for a heat pump in cooling and heating modes. A subsequent paper [35] indicates that the cyclic behavior of an air-

conditioning system will result in start-up losses. This is mainly due to the inability of the system to isolate the refrigerant during shutdown which leaves the condenser devoid of any refrigerant. This absence of refrigerant in the condenser at start-up will result in the flashing of the evaporator and a 15-20 second delay before the throttling device is flooded with liquid. This results in a subsequent delay in the cooling capacity buildup. Mulroy and Didion [36] and Kapadia and Sanjeev [37] conducted similar analysis on the start-up transients and they concluded that the losses are the maximum at the time of start-up and gradually reduce as the system approaches steady state conditions. Murphy and Goldschmidt's experimental analysis on the shutdown condition [34] has validated the point that both the temperature and pressure increase in the evaporator, which affects the conditions in the room. Tanaka et al. [38] studied the dynamic change of refrigerant quantity, along with the temperature and pressure variations. Based on their results, they suggested light design of heat pumps, with minimum refrigerant charge and preventing refrigerant flow during off cycle for improving the start-up performance. Wang and Wu [39] showed that the start-up transients are greatly influenced by the shutdown transients. Prevention of the refrigerant migration during shutdown by the use of a magnetic valve reduces the total power input during the start-up cycle by 4%. Li and Alleyne [40] were perhaps the only people to have simulated and validated a complete model of a vapor compression system for start-up/shutdown transients. They have achieved this using the MB approach of the heat exchangers. They have talked about the possible changes in states inside the heat exchanger during the off cycle and pictorially represented it in Figure 5.1. This thesis is different from the work done by Li and

Alleyne in the fact that this thesis aims to simulate and validate the start-up/shutdown transients for a more complex FCV model of the heat exchangers.
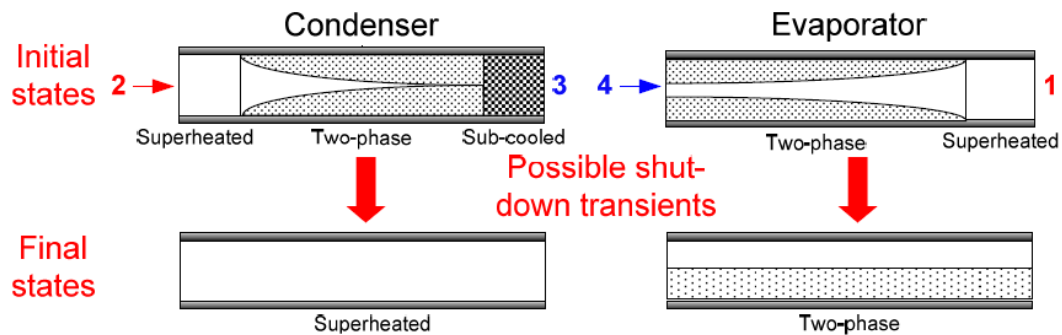
Figure 5.1 Possible Transient Behaviors in Compressor Shutdown Operations [40]

The rest of the section has been organized as follows: Subsection 5.1 deals with the changes made to the simulation models in order to run the simulations. Subsection 5.2 consists of the simulation results and their analysis. The validation results are presented in Subsection 5.3.

5.1 Simulation Models

The simulation models used here are similar to those explained in section 2 but a few changes have to be made in order for the models to work for the start-up/shutdown condition when the compressor is off and the mass flow rate of the refrigerant is zero. The major changes in the model are carried out with respect to the heat transfer coefficients. Following are the heat transfer correlations being used in the model currently and the reasons as to why some of them are not valid for start-up/shutdown:

- **Condensation correlation by Dobson[41] for two phase refrigerant**- During the shutdown scenario, the condition that arises in the condenser is that of film condensation. If the temperature of surface is below the saturation temperature of vapor, condensate will form on the surface and under the action of gravity will flow down. If the liquid wets the surface, a smooth film is formed, and the process is called film condensation. The Dobson correlation [41] is not valid for such a case because of its inability to handle zero mass flux. Chato introduced a new correlation [42] for film wise condensation which is given by Equation 5.1.

$$h_{cond} = 0.555 \left[\frac{\rho^2 g k^3 h_{fg}}{vd(T_{sat} - T_w)} \right]^{\frac{1}{4}} \qquad \qquad 5.1$$

- **Boiling correlation by Wattlet [43] for two phase refrigerant**- During the event of shutdown, the evaporator will be in the state of pool boiling. When a surface is exposed to a liquid and is maintained at a temperature above the saturation temperature of the liquid, boiling may occur, and the heat flux will depend on the difference in temperature between the surface and saturation temperature. When the heated surface is submerged below a free surface of liquid, the process is referred to as pool boiling. The Wattlet correlation accounts for this condition by incorporating two separate terms for pool boiling and convective boiling. Because of this reason, the correlation is valid even at the shutdown condition and hence does not require any change. The Wattlet correlation [43] for boiling is given by Equations 5.2 through 5.8.

$$h_{TP} = [h_{nb}^n + h_{cb}^n]^{\frac{1}{n}} \quad n = 2.5 \tag{5.2}$$

$$h_{nb} = 55q^{0.67}M^{-0.5}[-log_{10}Pr]^{-0.55}[Pr]^{0.12} \tag{5.3}$$

$$h_{cb} = Fh_l R \tag{5.4}$$

$$F = 1 + 1.925X_{tt}^{-0.83} \tag{5.5}$$

$$h_l = \frac{0.023k_l}{D}Re_l^{0.8}Pr_l^{0.4} \tag{5.6}$$

$$R = 1.32Fr_l^{0.2}, for \; Fr_l < 0.25 \tag{5.7}$$

$$R = 1, for \; Fr_l \geq 0.25 \tag{5.8}$$

- **Air side convection correlation by Colburn [44]** - During the condition when the fans are off at shutdown, the condition that arises is that of free convection. Natural/Free convection is a result of the motion of the fluid due to density changes arising from the heating process. A hot radiator for heating the room is an example of a practical device which transfers heat by free convection. Colburn factor correlation is not valid for the free convection condition because it cannot handle zero mass flow rate of air. This problem can be overcome by introducing the free convection heat transfer correlation by Churchill and Chu[45] given by Equations 5.9 and 5.10.

$$Nu^{\frac{1}{2}} = 0.6 + 0.387\left\{\frac{Gr * Pr}{\left[\left[1 + \left(\frac{0.559}{Pr}\right)^{\frac{9}{16}}\right]^{\frac{16}{9}}\right]}\right\}^{\frac{1}{6}} \tag{5.9}$$

$$h_{conv} = Nu * \frac{k}{L} \qquad\qquad 5.10$$

The film wise condensation and free convection heat transfer correlations are incorporated into the model and these values are compared to the heat transfer coefficient values at the instant when the system is running and the maximum of those two values is selected as the value of the heat transfer coefficient for that particular instant.

5.2 Simulation Results

The first attempt to the simulation and validation of start-up and shutdown transients in a vapor compression cycle has been carried out by Li and Alleyne [40]. They have developed a dynamic model of a vapor compression cycle and the validation results were presented for two scenarios: stop-start steps in both compressor speed and valve opening inputs; only stop-start step changes in the compressor speed input. These results demonstrate that the switched heat exchanger modeling is a reasonable and valuable approach to describe transient behaviors for VCC systems. In a similar analysis, this Subsection of the thesis focuses on the simulation results of the FCV models for the four test cases shown in the Table 5.1. The test cases in Table 5.1 are related to the shutdown transients. The start-up transients are simulated by turning on the compressor after the above simulations have reached equilibrium state.

Table 5.1 Start-up/Shutdown Simulation Cases

	During off cycle	
Compressor Sequence	**Valve**	**Fans**
On-Off-On	EEV open	On
On-Off-On	EEV closed	On
On-Off-On	EEV open	Off
On-Off-On	EEV closed	Off

5.2.1 Shutdown Condition of Valve Open and Fans On

In this start-up/shutdown scenario, the compressor is switched off to replicate the shutdown condition while the valve remains open and the fans remain on during the off cycle. One of the inputs to the model is the speed of the compressor and is given a step signal from its initial operating condition value to zero. Once the compressor is switched off, the value of mass flux becomes zero and the condensation heat transfer correlation switches to its film condensation value while the air side heat transfer correlation maintains its original steady state value since the fans have not been switched off. The simulation results for this case are shown in Figure 5.2.
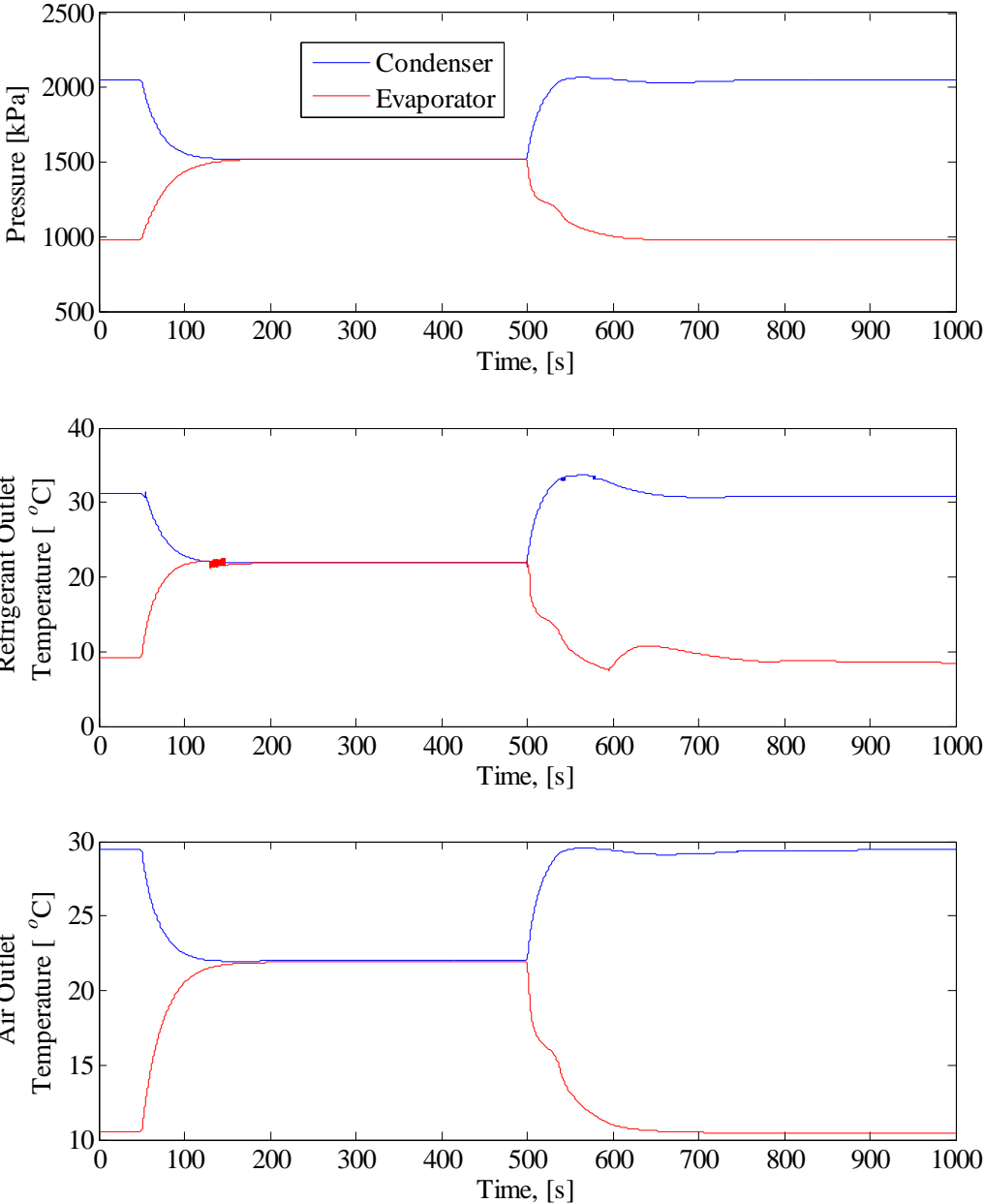
Figure 5.2 Simulation Start-up/Shutdown for the Condition of Valve Open and Fans On at Shutdown

5.2.2 Shutdown Condition of Valve Closed and Fans On

In this start-up/shutdown scenario, the compressor is switched off and the valve is closed simultaneously at shutdown while the fans remain on. Step inputs are given to the compressor speed and valve command to replicate the shutdown scenario. From the results shown in Figure 5.3, the transient in the evaporator refrigerant temperature at start-up is because of the splashing of the refrigerant explained in detail by Murphy and Goldschmidt [35].

5.2.3 Shutdown Condition of Valve Open and Fans Off

In this start-up/shutdown scenario, the compressor and the fans are switched off simultaneously while the valve remains open. Switching off the fans at shutdown is simulated by giving a step input to the mass flow rate of the air from its initial steady state value to zero. In this case, since the fans are also switched off, the air-side heat transfer coefficient value will be got from the free convection heat transfer correlation discussed in Subsection 5.1. The simulation results for this case are shown in Figure 5.4.

5.2.4 Shutdown Condition of Valve Closed and Fans Off

In this start-up/shutdown scenario, the compressor and the fans are switched off simultaneously and the valve is closed. Switching off the fans at shutdown is simulated by giving a step input to the mass flow rate of the air from its initial steady state value to zero. As can be seen from Figure 5.5, the pressures and temperatures take a long time to reach their corresponding ambient values. This is because, when the valve is closed, all

the components in the system are isolated from each other and since the fans are also off, there is no appreciable heat transfer and hence the slow transient of the temperatures and pressures at shutdown.
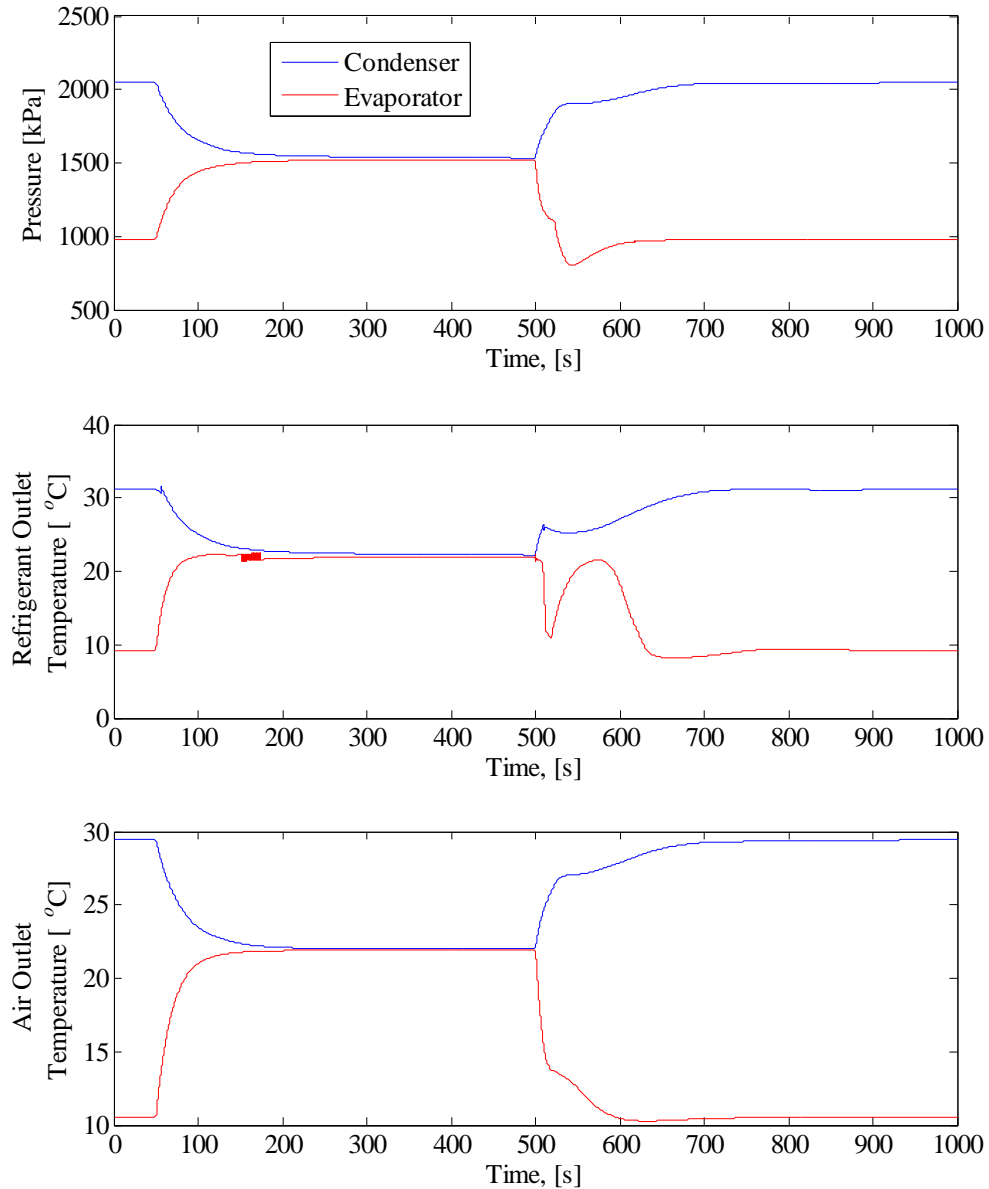

Figure 5.3 Simulation Start-up/Shutdown for the Condition of Valve Closed and Fans On at Shutdown
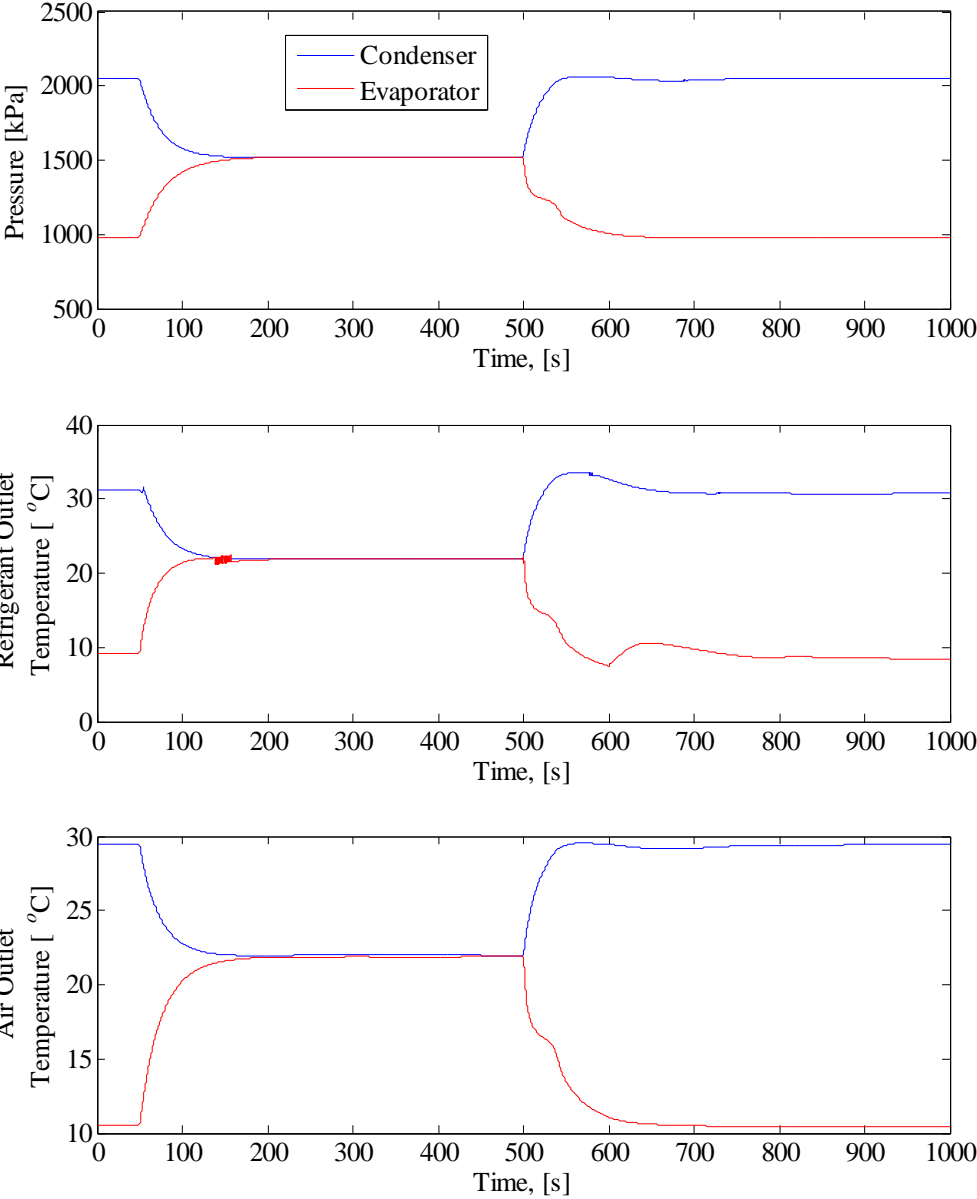
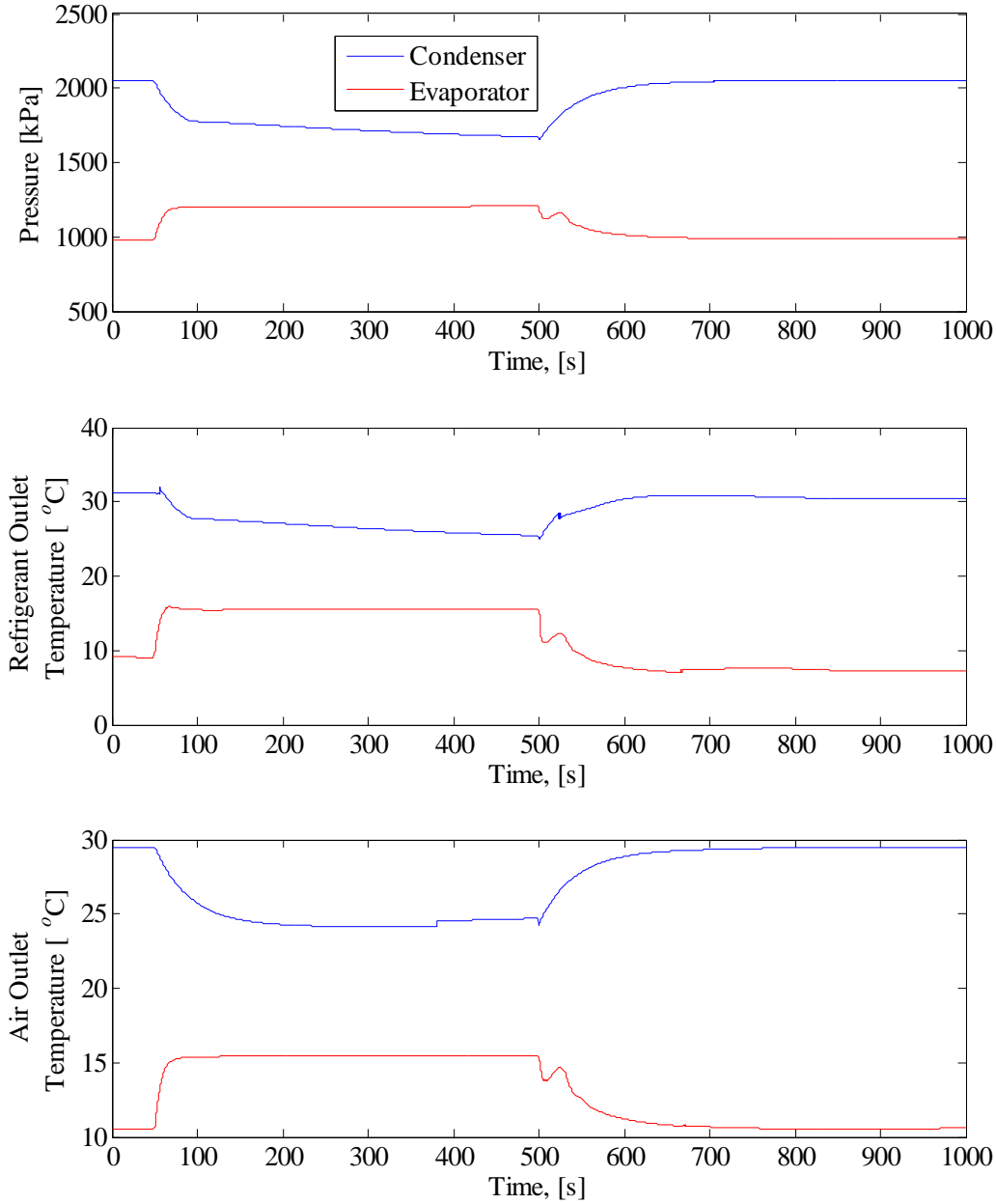**Figure 5.4 Simulation Start-up/Shutdown for the Condition of Valve Open and Fans Off at Shutdown**

Figure 5.5 Simulation Start-up/Shutdowns for the Condition of Valve Closed and Fans Off at Shutdown

5.3 Validation Results

Two of the above four start-up/shutdown scenarios have been chosen to demonstrate the capability of the finite control volume approach for various operating conditions. Here, the results are validated for the same experimental system described in Section 3.

5.3.1 Shutdown Condition of Valve Open and Fans Off

This shutdown condition has been implemented on the experimental system by giving a step command to the evaporator and condenser fans along with the compressor speed while keeping the valve position constant. The initial validation results of the pressures and refrigerant outlet temperatures for this shutdown condition are shown in Figure 5.6. As can be seen from Figure 5.6(d), the refrigerant temperature at the evaporator outlet does not seem to match well during the start-up. In order to solve this problem, several possible solutions were looked at. The first of these cases was modeling a receiver. The experimental system consists of a receiver as seen in Figure 3.2. But, the simulation model consists of only the four basic components of evaporator, condenser, expansion valve and compressor. Since the transients of the condenser parameters for both simulation and experiment agreed with each other, the receiver was modeled by assuming the fact that the condenser was perfect. Since the outlet of an ideal receiver is always a saturated liquid, the enthalpy to the inlet of the valve i.e. the enthalpy at the outlet of the receiver is calculated by using the fluid property tables and experimental condenser pressure. The model was run and validated for this condition of an ideal

receiver and the results of the evaporator refrigerant outlet temperature were compared as shown in Figure 5.7. As can be seen from (a) and (b) in Figure 5.7, the introduction of a receiver has definitely improved the start-up transients of the evaporator refrigerant outlet temperature. But still, in this case as well, the start-up transient in the simulation is slower than that in the experiment.
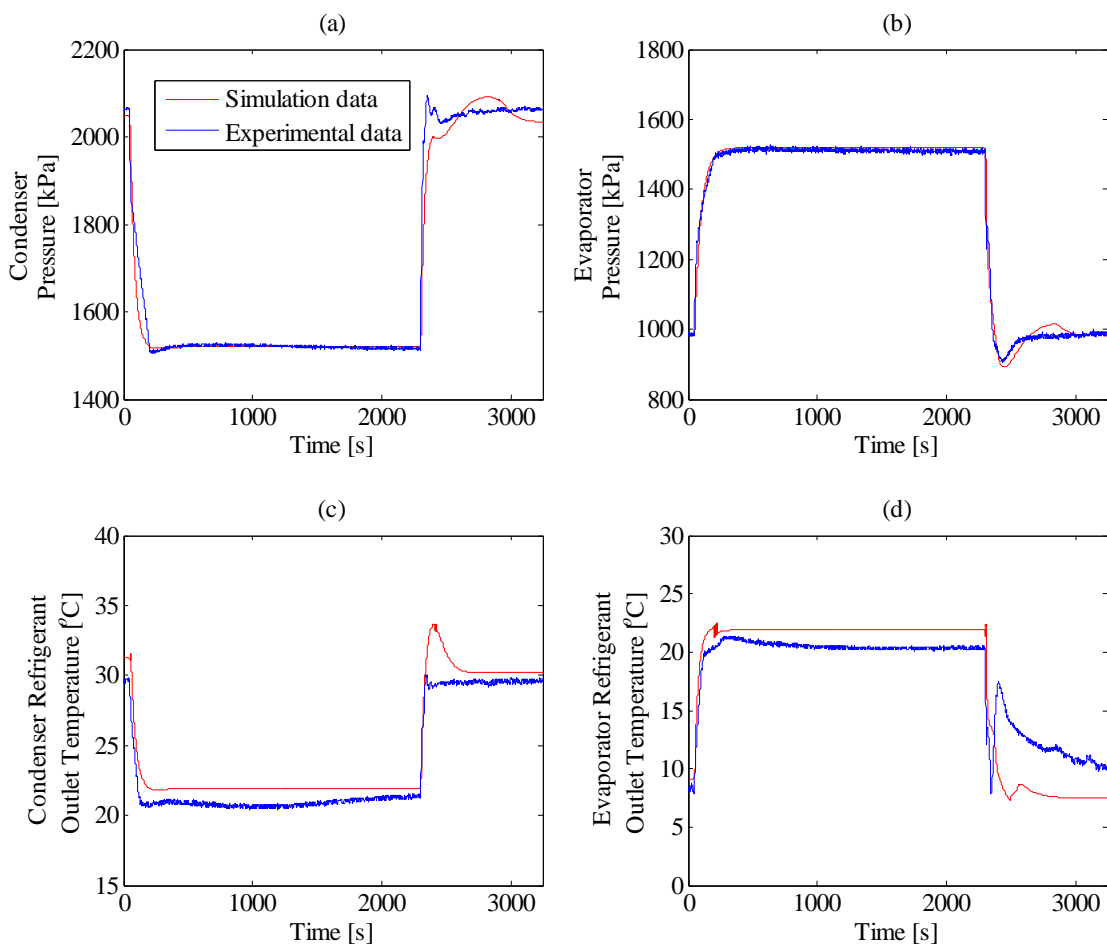
Figure 5.6 Initial Results for Validation of Shutdown Condition of Valve Open, Fans Off

Result for the condition with no receiver (a)

Result for the condition with receiver (b)
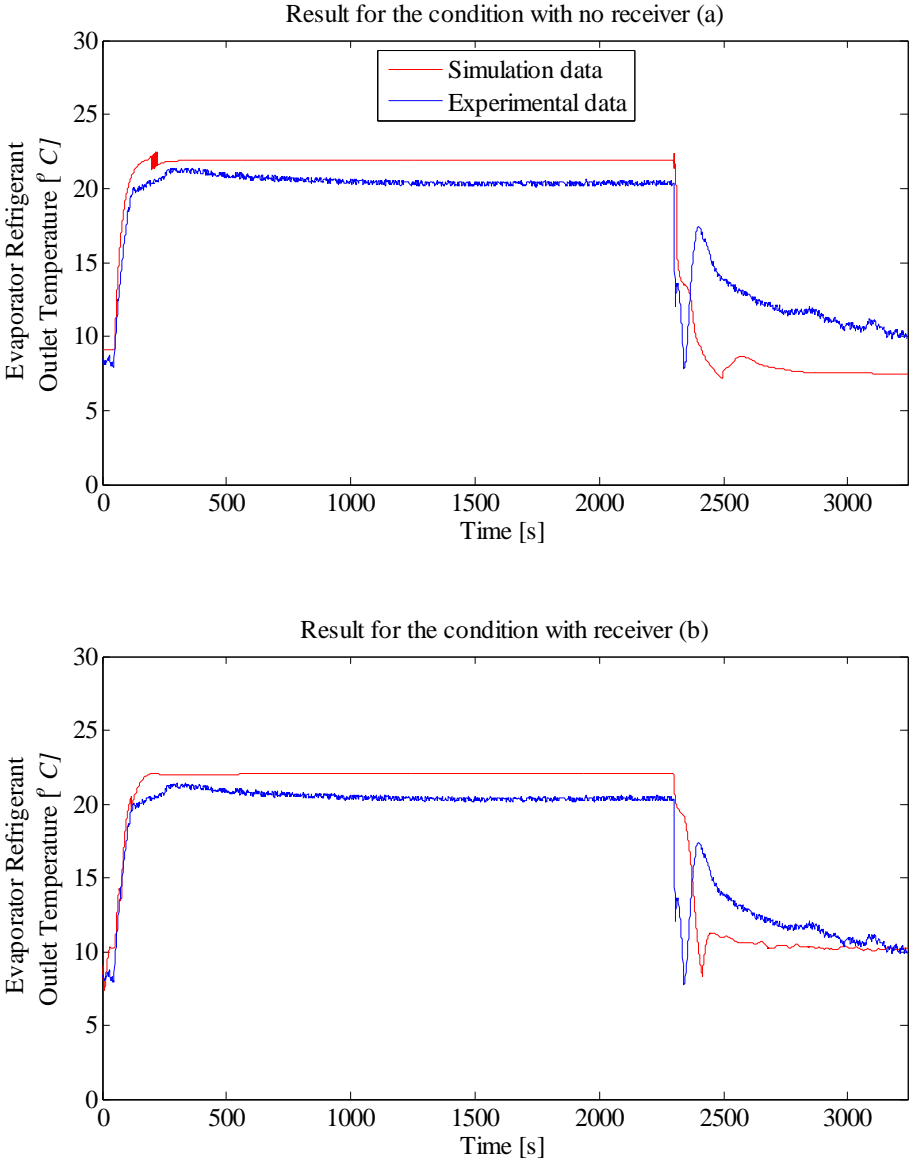
Figure 5.7 Comparison of Evaporator Refrigerant Outlet Temperatures

The second possible solution that was looked at is changing the value of slip ratio to speed up the dynamics of the transients. Slip ratio is defined as the ratio of the velocities of the vapor and liquid phases in a two-phase flow. The acceptable limits for

the slip ratio are 1 and $\left(\dfrac{\rho_f}{\rho_g}\right)^{\frac{1}{3}}$ given by homogenous and Zivi correlation respectively

[3]. Since slip ratio is a tunable parameter with no means to physically calculate it using the experimental set-up, this was a reasonable solution to look at. So the initial model (without the receiver) was taken and the slip ratio was tuned within the limits specified to achieve a better start-up response. The final results for this condition are shown in Figures 5.8 and 5.9. Since the fans are off during shutdown, there is no flow of air and hence the validation of air temperatures during shutdown is not a correct result. This is represented by the hatched section in Figure 5.8.

As can be seen, this solution yields results better than the one with the receiver. Still, there is a slight discrepancy in the start-up transient concerning the evaporator refrigerant outlet temperature in Figure 5.9 (d). This might be because of the fact that the condenser is completely dry at start-up and it takes some time for it to throttle liquid instead of vapor [35]. This leads to flashing of the vapor immediately after start-up which agrees with the results from experiment and simulation. The greater increase in the temperature value immediately after the flashing phenomena in the experiment can be attributed to the fact that the condenser takes a longer time to throttle liquid instead of vapor. Also, there is a possibility of the refrigerant entrained in the oil inside the compressor during the shutdown process. When the system is started up, it takes time for the refrigerant to completely separate from the oil which might be the reason for the slow transient nature of the evaporator refrigerant outlet temperature during start-up. The models are not built to handle the mixing of the refrigerant and oil and hence this

transient is not accounted for in the simulation results. All these explanations can be attributed for the slight discrepancy in the experimental and simulation results in Figure 5.9 (d).
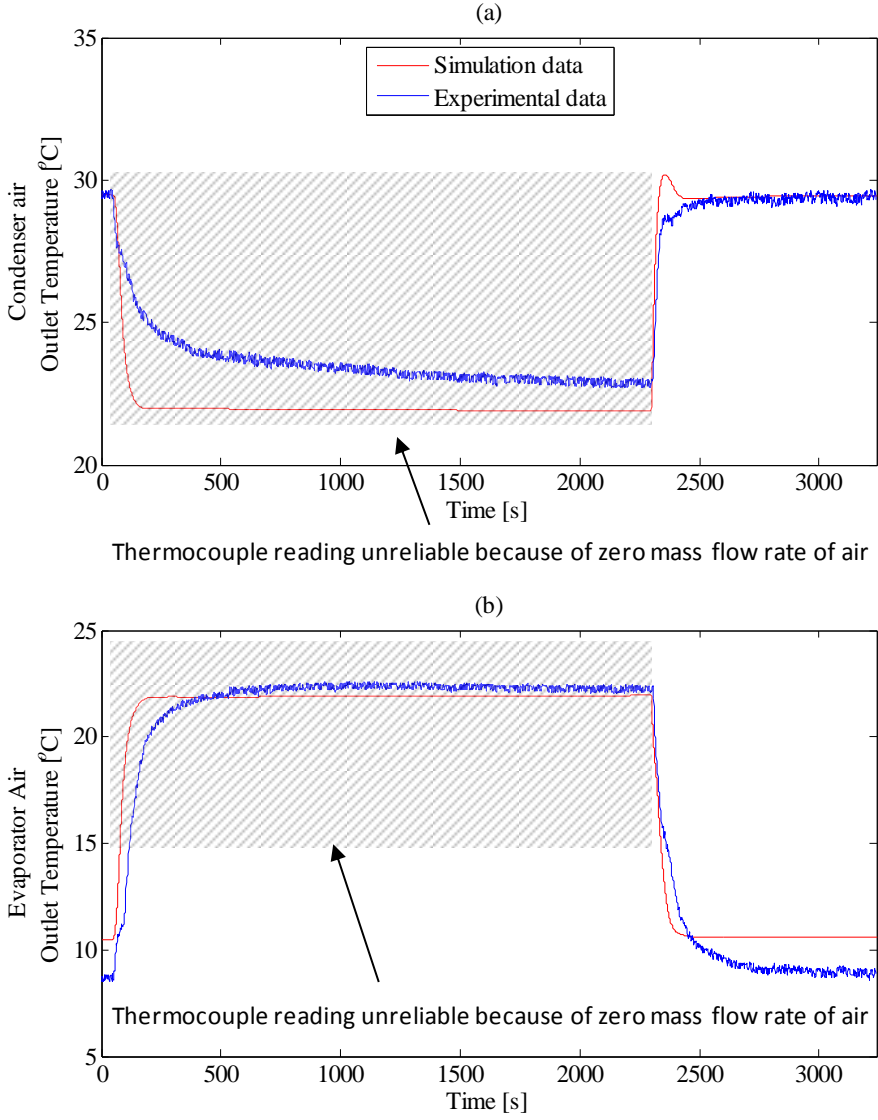

Figure 5.8 Validation Results of Air Outlet Temperatures for the Shutdown Condition of Valve Open and Fans Off

Figure 5.9 Validation Results of Pressures and Refrigerant Outlet Temperatures for the Shutdown Condition of Valve Open and Fans Off

5.3.2 Shutdown Condition of Valve Closed and Fans Off

The shutdown condition has been implemented on the experimental system by giving a step command to the valve opening signal as well the evaporator and condenser fans along with the speed of the compressor. The validation results for the above condition are shown in Figures 5.10 and 5.11. In the experimental system, the thermocouple values of refrigerant and air temperatures at the condenser and evaporator

outlet are only meaningful when the mass flow rate of the refrigerant and air are greater than zero. Since, in this condition of the valve closed and fans off during shutdown, there is no flow of refrigerant and air through the system and validation of temperatures
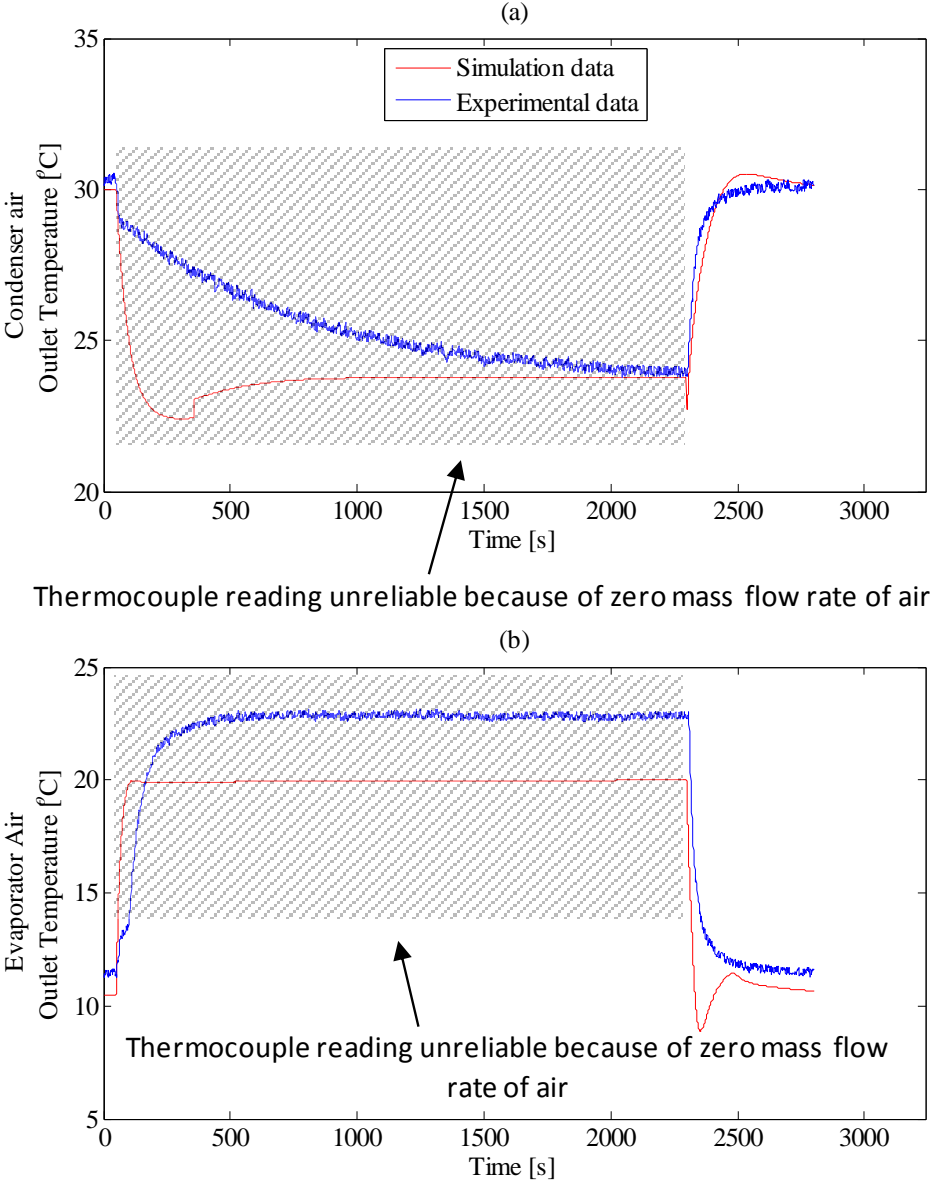
Figure 5.10 Validation Results of the Air Outlet Temperatures for the Shutdown Condition of Valve Closed and Fans Off

at shutdown is not a correct idea. The slight discrepancy of the air and refrigerant temperatures upon start-up can be attributed to the thermal inertia of the ducting in the experimental system. The simulation models do not take this concept into account. This area is represented by hatched section in Figures 5.10 and 5.11.
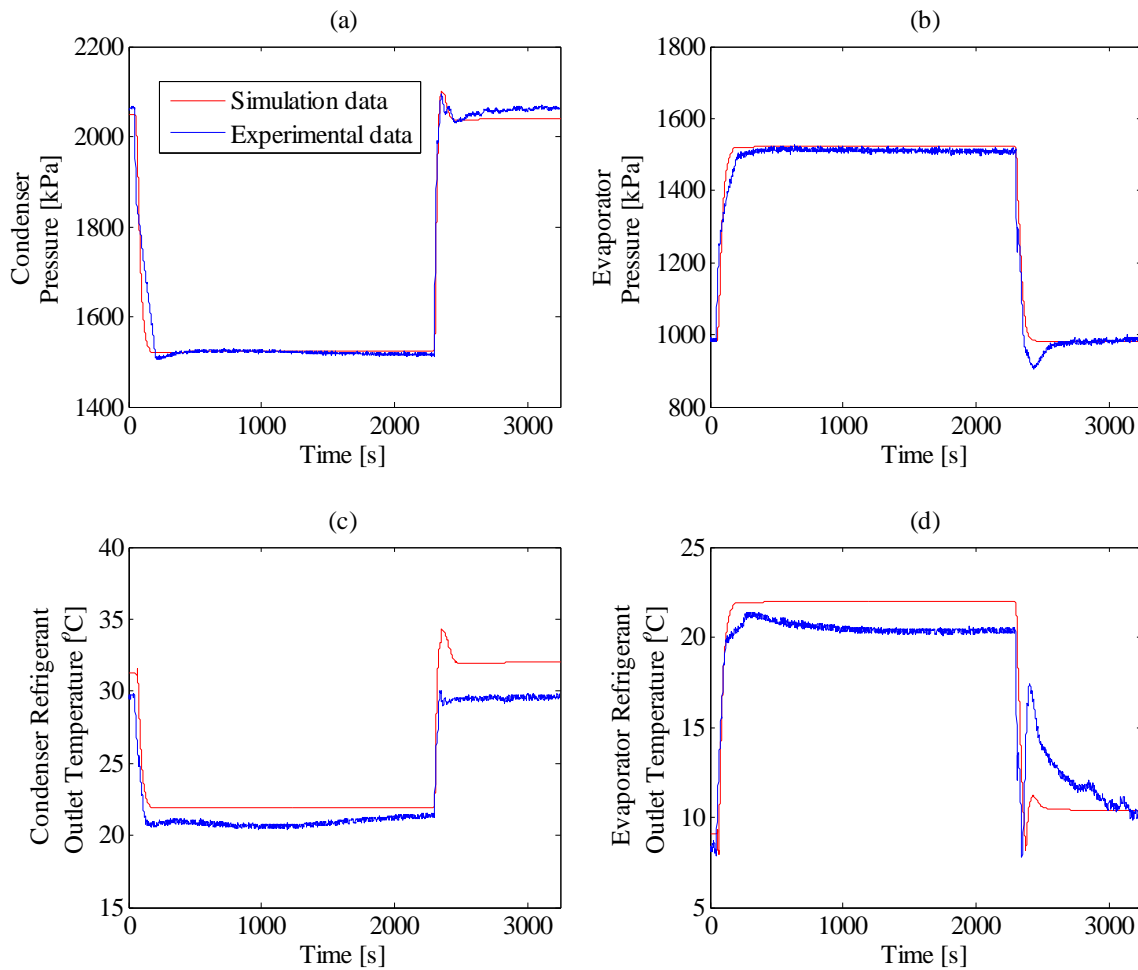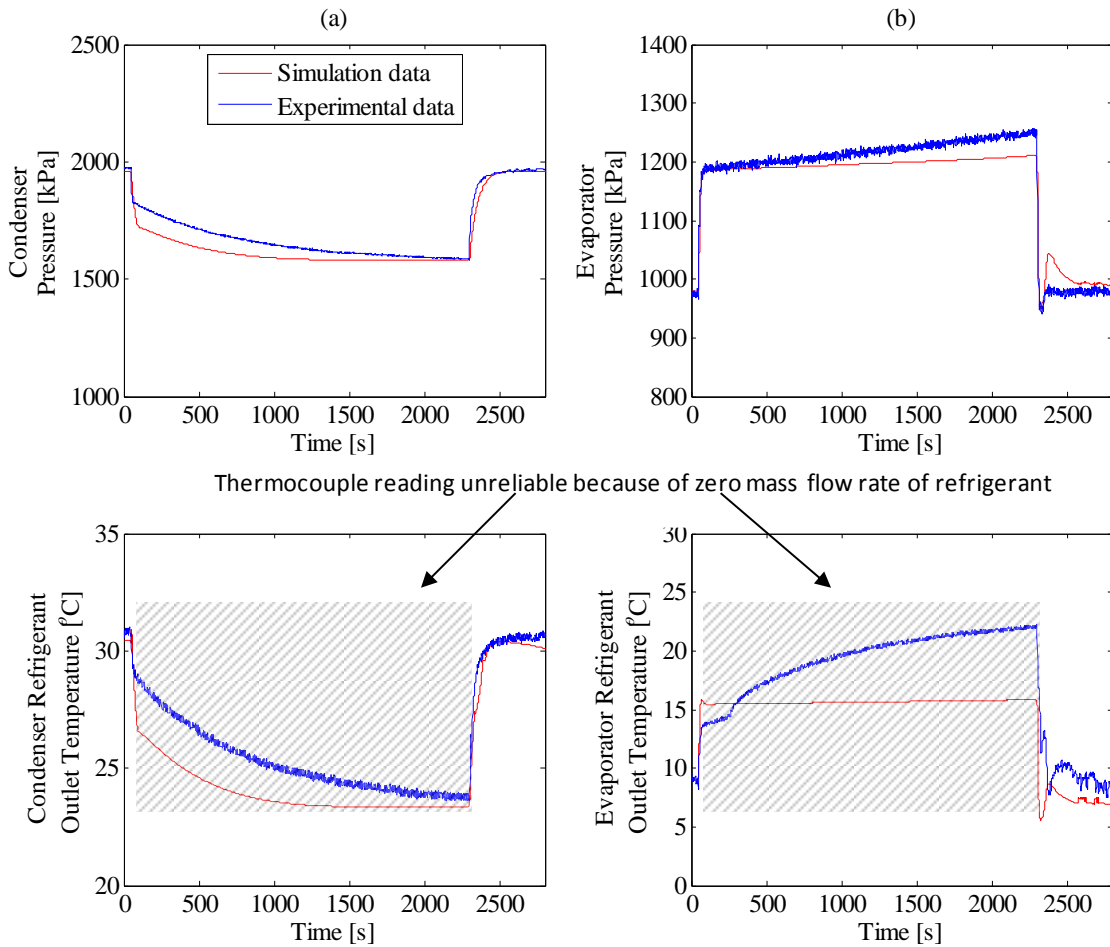

Figure 5.11 Validation Results of the Pressures and Refrigerant Outlet Temperatures for the Shutdown Condition of Valve Closed and Fans Off

6. CONCLUSION AND FUTURE WORK

This research makes several contributions to the field of AC&R modeling. The existing FCV models have been modified to run the simulations related to fault and start-up/shutdown transients. These results have been validated against the experimental data.

Modifications have been made to the experimental system to replicate the vapor compression system faults like introducing a pilot valve in between the suction and discharge lines to simulate the compressor leakage fault. Operating conditions in the model have been changed to match those of the experiment and simulations carried out to match the experimental fault scenario. Prior work in this area had only the simulation results for various faults in vapor compression system with limited validation results. The present study overcomes this limitation.

Major change in the models has been made for the analysis of start-up and shutdown transients. To overcome the limitations of the model not working for the conditions of zero mass flux and zero air flow velocity during shutdown, the heat transfer correlations for condensation and convection have been modified to accommodate for the conditions of film condensation and free convection respectively. An analysis of the simulation and validation of start-up/shutdown transients has been carried out by Li and Alleyne [40] using moving boundary modeling of the heat exchangers. Their validation results are based on the surface measurements of the refrigerant outlet temperature. This kind of measurement may not be accurate due to the fact that the thermocouple might not be able to effectively capture the refrigerant dynamics. This thesis overcomes the above problem by validating the refrigerant

temperatures where the thermocouples are placed in-line with the refrigerant in the experimental system.

In the present work, we take into consideration a simple vapor compression system with the general four components of evaporator, condenser, compressor and EEV. In general, some air-conditioning systems have additional components like receiver, accumulator, extra evaporator etc. Moreover not all systems have EEV installed. Some of those might be using a Thermo Static Expansion Valve (TXV). Future research might look into modeling these components and obtain the simulation and validation results for the faults as well as start-up/shutdown transients. This will definitely increase the scope of simulating results for different types of air-conditioning systems.

REFERENCES

[1]   U.S Department of Energy, 2011, Energy savers: Space heating and cooling [Online]. Available: http://www.energysavers.gov/your_home/space_heating_cooling/index.cfm/mytopic=12300

[2]   Energy Information Administration, 2009, International Energy Outlook 2009 [Online]. Available: http://www.eia.doe.gov/oiaf/ieo/world.html

[3]   A. Gupta, "Reduced order modeling of heat exchangers using high order finite control volume models," Masters' thesis, Texas A&M University, College Station, TX, 2007.

[4]   S. Bendapudi, J. E. Braun, and E. A. Groll, "A comparison of moving-boundary and finite-volume formulations for transients in centrifugal chillers," *International Journal of Refrigeration,* vol. 31, pp. 1437-1452, 2008.

[5]   T. L. Hemami, and W. E. Dunn, "Development of a transient system model of mobile air-conditioning systems," Masters' thesis, University of Illinois, Urbana Champaign, IL, 1998.

[6]   M. Dhar, "Transient analysis of refrigeration system," Ph.D dissertation, Purdue University, West Lafayette, IN, 1978.

[7]   W. D. Gruhle and R. Isermann, "Modeling and control of a refrigerant evaporator," *Journal of Dynamic Systems, Measurement, and Control,* vol. 107, pp. 235-240, 1985.

[8]   J. Chi and D. Didion, "A simulation model of the transient performance of a heat pump," *International Journal of Refrigeration,* vol. 5, pp. 176-184, 1982.

[9]   J. W. MacArthur and E. W. Grald, "Prediction of cyclic heat pump performance with a fully distributed model and a comparison with experimental data," *ASHRAE Trans.*, vol. 93, pp. 1159-1178, 1987.

[10]   P. Mithraratne, N. E. Wijeysundera, and T. Y. Bong, "Dynamic simulation of a thermostatically controlled counter-flow evaporatorsimulation dynamique d'un évaporateur à détendeur thermostatique avec débit à contre-courant," *International Journal of Refrigeration,* vol. 23, pp. 174-189, 2000.

[11]   G. L. Wedekind, B. L. Bhatt, and B. T. Beck, "A system mean void fraction model for predicting various transient phenomena associated with two-phase evaporating and condensing flows," *International Journal of Multiphase Flow,* vol. 4, pp. 97-114, 1978.

[12]   D. E. Stouppe and Y. S. Lau, "Air conditioning and refrigeration equipment failures," *National Engineer,* vol. 93, pp. 14–17, 1989.

[13]   M. S. Breuker and J. E. Braun, "Demonstration of a statistical, rule-based fault detection and diagnostic method on a rooftop air conditioning unit," in *CLIMA 2000 Conference Proceedings*, 1997: CD-ROM.

[14]   M. C. Comstock, J. E. Braun, and E. A. Groll, "A survey of common faults for chillers," *ASHRAE Trans.,* vol. 108, pp. 819-825, 2002.

[15]   M. G. McKellar, "Failure diagnosis for a household refrigerator," Masters' thesis, Purdue University, West Lafayette, IN, 1987.

[16] L. A. Stallard, "Model based expert system for failure detection and identification of household refrigerators," Masters' thesis, Purdue University, West Lafayette, IN, 1989.

[17] J. Wagner and R. Shoureshi, "Failure detection diagnostics for thermofluid systems," *Journal of Dynamic Systems, Measurement, and Control,* vol. 114, pp. 699-706, 1992.

[18] H. T. Grimmelius, J. K. Woud, and G. Been, "Online failure diagnosis for compression refrigeration plants," *International Journal of Refrigeration-Revue Internationale Du Froid,* vol. 18, pp. 31-41, Jan 1995.

[19] M. Stylianou and D. Nikanpour, "Performance monitoring, fault detection, and diagnosis of reciprocating chillers," *ASHRAE Transactions,* vol. 102, pp. 615-627, 1996.

[20] T. M. Rossi and J. E. Braun, "A statistical, rule-based fault detection and diagnostic method for vapor compression air conditioners," *HVAC&R Research,* vol. 3, pp. 19-37, 1997.

[21] M. C. Keir, "Dynamic modeling, control, and fault detection in vapor compression systems " Masters' thesis, University of Illinois, Urbana-Champaign, 2006.

[22] N. Epstein, "Fouling of heat exchangers," in *Sixth International Heat Transfer Conference*, 1978, pp. 235-253.

[23] J. A. Siegel and W. W. Nazaroff, "Predicting particle deposition on HVAC heat exchangers," *Atmospheric Environment,* vol. 37, pp. 5587-5596, 2003.

[24] B. Wilhelmsson, "Consider spiral heat exchangers for fouling application," *Hydrocarbon Processing,* vol. 84, pp. 81-83, 2005.

[25] M. Kim and M. S. Kim, "Performance investigation of a variable speed vapor compression system for fault detection and diagnosis," *International Journal of Refrigeration,* vol. 28, pp. 481–488, 2005.

[26] M. S. Breuker and J. E. Braun, "Common faults and their impacts for rooftop air conditioners," *HVAC&R Research,* vol. 4, pp. 303-318, Jul 1998.

[27] C. Thybo, B. D. Rasmussen, and R. Izadi-Zamanabadi, "Detecting air circulation faults in refrigerated display cabinets," in *Proc. of the IIF - IIR Commission D1/B1*, 2002, pp. 211-217.

[28] W. M. Kays and A. L. London, *Compact Heat Exchangers*. New York: McGraw-Hill Book Company, 1984.

[29] S. N. Kondepudi and D. L. O'Neal, "Performance of finned-tube heat exchangers under frosting conditions: I. Simulation model," *International Journal of Refrigeration,* vol. 16, pp. 175-180, 1993.

[30] Y. Yao, Y. Jiang, S. Deng, and Z. Ma, "A study on the performance of the airside heat exchanger under frosting in an air source heat pump water heater/chiller unit," *International Journal of Heat and Mass Transfer,* vol. 47, pp. 3745-3756, 2004.

[31] S. Bendapudi and J. E. Braun, "A review of literature on dynamic models of vapor compression equipment, " *ASHRAE Report*, No. 4036-5, 2002.

[32] V. W. Goldschmidt and W. E. Murphy, "Transient performance of air conditioners," in *New Zealand Institution Engineers (NZIE) Proceedings*, 1974, pp. 715-738.

[33] J. Judge. (1996). "Transient and steady state study of pure and mixed refrigerants in a residential heat pump, " *[electronic resource]*. Available: http://nla.gov.au/nla.cat-vn3828715

[34] W. E. Murphy and V. W. Goldschmidt, "Cycling characteristics of a residential air conditioner-modeling of shutdown transients," *ASHRAE Trans.,* vol. 92, pp. 186-202, 1986.

[35] W. E. Murphy and V. W. Goldschmidt, "Transient response of air conditioners: A qualitative interpretation through a sample case," *ASHRAE Trans.*, vol. 90, pp. 997-1008, 1984.

[36] W. J. Mulroy and D. A. Didion, "Refrigerant migration in a split-unit air conditioner," *ASHRAE Trans.*, vol. 91, pp. 193-206, 1985.

[37] R. G. Kapadia, S. Jain, and R. S. Agarwal, "Transient characteristics of split air-conditioning systems using R-22 and R-410a as refrigerants," *HVAC&R Research,* vol. 15, pp. 617 - 649, 2009.

[38] N. Tanaka, M. Ikeuchi, and G. Yamanaka, "Experimental study on the dynamic characteristics of a heat pump," *ASHRAE Trans.,* vol. 88, pp. 323-331, 1982.

[39] W. Jun and W. Yezheng, "Start-up and shut-down operation in a reciprocating compressor refrigeration system with capillary tubes," *International Journal of Refrigeration,* vol. 13, pp. 187-190, 1990.

[40] B. Li and A. G. Alleyne, "A dynamic model of a vapor compression cycle with shut-down and start-up operations," International Journal of Refrigeration, vol. 33, pp. 538-552, 2010.

[41] M. K. Dobson and J. C. Chato, "Condensation in smooth horizontal tubes," Journal of Heat Transfer, vol. 120, pp. 193-213, 1998.

[42] J. C. Chato, "Laminar condensation inside horizontal and inclined tubes," *ASHRAE,* vol. 4, pp. 52–60, 1962.

[43] J. P. Wattelet, J. C. Chato, A. L. Souza, and B. R. Christoffersen, "Evaporative characteristics of R-12, R-134a, and a mixture at low mass fluxes," vol. 100, pp. 603-615, 1994.

[44] A. P. Colburn, "A method of correlating forced convection heat-transfer data and a comparison with fluid friction," *International Journal of Heat and Mass Transfer,* vol. 7, pp. 1359-1384, 1964.

[45] J. P. Holman, *Heat Transfer*, Nineth ed.: McGraw-Hill, New York, 2002.

APPENDIX

Conservation of Refrigerant Energy:

$$\dot{U} = \dot{H}_{in} - \dot{H}_{out} + \dot{Q}_w \qquad\qquad 1$$

$$\dot{H} = \dot{m} \cdot h \qquad\qquad 2$$

$$\dot{Q}_w = \alpha_i A_i (T_w - T_r) \qquad\qquad 3$$

$$\begin{bmatrix} \dot{U}_1 \\ \vdots \\ \dot{U}_k \\ \vdots \\ \dot{U}_n \end{bmatrix} = \begin{bmatrix} \dot{m}_{in} h_{in} - \dot{m}_1 h_1 + \alpha_{i,1} A_{i,1} (T_{w,1} - T_{r,1}) \\ \vdots \\ \dot{m}_{k-1} h_{k-1} - \dot{m}_k h_k + \alpha_{i,k} A_{i,k} (T_{w,k} - T_{r,k}) \\ \vdots \\ \dot{m}_{n-1} h_{n-1} - \dot{m}_{out} h_{out} + \alpha_{i,n} A_{i,n} (T_{w,n} - T_{r,n}) \end{bmatrix} \qquad\qquad 4$$

Conservation of Refrigerant Mass:

$$\begin{bmatrix} \dot{m}_{e,1} \\ \vdots \\ \dot{m}_{e,k} \\ \vdots \\ \dot{m}_{e,n} \end{bmatrix} = \begin{bmatrix} \dot{m}_{in} - \dot{m}_1 \\ \vdots \\ \dot{m}_{k-1} - \dot{m}_k \\ \vdots \\ \dot{m}_{n-1} - \dot{m}_{out} \end{bmatrix} \qquad\qquad 5$$

$$\dot{m}_e = \dot{m}_{in} - \dot{m}_{out} \qquad\qquad 6$$

Conservation of Tube-wall Energy:

$$\dot{E}_w = \dot{Q}_a - \dot{Q}_w \qquad\qquad 7$$

$$\dot{Q}_a = \alpha_o A_o (T_a - T_w) \qquad\qquad 8$$

$$
\begin{bmatrix} \dot{E}_{w,1} \\ \vdots \\ \dot{E}_{w,k} \\ \vdots \\ \dot{E}_{w,n} \end{bmatrix} = \begin{bmatrix} \alpha_{o,1}A_{o,1}(T_{a,1} - T_{w,1}) - \alpha_{i,1}A_{i,1}(T_{w,1} - T_{r,1}) \\ \vdots \\ \alpha_{o,k}A_{o,k}(T_{a,k} - T_{w,k}) - \alpha_{i,k}A_{i,k}(T_{w,k} - T_{r,k}) \\ \vdots \\ \alpha_{o,n}A_{o,n}(T_{a,n} - T_{w,n}) - \alpha_{i,n}A_{i,n}(T_{w,n} - T_{r,n}) \end{bmatrix} \qquad 9
$$

Governing Differential Equations:

Combining the Equations 4, 6 and 9, we get a single vector as given by Equation 10. Equation 11 gives the internal energy of the refrigerant where, $m_{e,k}$ and $u_{e,k}$ are the mass of the refrigerant and the average internal energy of refrigerant. The time derivative of the internal energy is given by Equation 12. Using the average refrigerant density $\rho_{e,k}$ and the Volume of the kth control region as $V_{e,k}$, the mass of the refrigerant in the kth control region is given by in Equation 13. The density and the internal energy can be written in terms of pressure, P_e and enthalpy, $h_{e,k}$ and their respective time derivatives are written as shown in Equation 15. The enthalpy $h_{e,k}$ from Equation 16 is substituted in Equation 15 to get Equation 17. The partial derivatives in Equations 18 and 19 are then used to obtain Equation 21. Conservation of mass Equation in Equation 22 is expanded using the same principle to get Equation 23. The tube wall energy is then expressed as a product of thermal capacitance and the lumped parameter wall temperature in Equation 24. This helps in getting the time derivative of the same as in Equation 25.

$$\begin{bmatrix} \dot{U}_1 \\ \vdots \\ \dot{U}_k \\ \vdots \\ \dot{U}_n \\ \dot{m}_e \\ \dot{E}_{w,1} \\ \vdots \\ \dot{E}_{w,k} \\ \vdots \\ \dot{E}_{w,n} \end{bmatrix} = \begin{bmatrix} \dot{m}_{in} h_{in} - \dot{m}_1 h_1 + \alpha_{i,1} A_{i,1} \left(T_{w,1} - T_{r,1} \right) \\ \vdots \\ \dot{m}_{k-1} h_{k-1} - \dot{m}_k h_k + \alpha_{i,k} A_{i,k} \left(T_{w,k} - T_{r,k} \right) \\ \vdots \\ \dot{m}_{n-1} h_{n-1} - \dot{m}_{out} h_{out} + \alpha_{i,n} A_{i,n} \left(T_{w,n} - T_{r,n} \right) \\ \dot{m}_{in} - \dot{m}_{out} \\ \alpha_{o,1} A_{o,1} \left(T_{a,1} - T_{w,1} \right) - \alpha_{i,1} A_{i,1} \left(T_{w,1} - T_{r,1} \right) \\ \vdots \\ \alpha_{o,k} A_{o,k} \left(T_{a,k} - T_{w,k} \right) - \alpha_{i,k} A_{i,k} \left(T_{w,k} - T_{r,k} \right) \\ \vdots \\ \alpha_{o,n} A_{o,n} \left(T_{a,n} - T_{w,n} \right) - \alpha_{i,n} A_{i,n} \left(T_{w,n} - T_{r,n} \right) \end{bmatrix} \qquad 10$$

$$U_{e,k} = m_{e,k} . u_{e,k} \qquad 11$$

$$\dot{U}_{e,k} = \dot{m}_{e,k} . u_{e,k} + m_{e,k} . \dot{u}_{e,k} \qquad 12$$

$$m_{e,k} = V_{e,k} . \rho_{e,k} \qquad 13$$

$$\dot{U}_{e,k} = V_{e,k} \left(\dot{\rho}_{e,k} . u_{e,k} + \rho_{e,k} . \dot{u}_{e,k} \right) \qquad 14$$

$$\dot{U}_{e,k} = V_{e,k} \left[\left(\left(\frac{\partial \rho_{e,k}}{\partial P_e} \bigg|_{h_{e,k}} \right) \dot{P}_e + \left(\frac{\partial \rho_{e,k}}{\partial h_{e,k}} \bigg|_{P_e} \right) \dot{h}_{e,k} \right) u_{e,k} \right.$$
$$\left. + \left(\left(\frac{\partial u_{e,k}}{\partial P_e} \bigg|_{h_{e,k}} \right) \dot{P}_e + \left(\frac{\partial u_{e,k}}{\partial h_{e,k}} \bigg|_{P_e} \right) \dot{h}_{e,k} \right) \rho_{e,k} \right] \qquad 15$$

$$h_{e,k} = u_{e,k} + \frac{P_e}{\rho_{e,k}} \qquad 16$$

$$\dot{U}_{e,k} = V_{e,k} \left[\left(\left(\frac{\partial \rho_{e,k}}{\partial P_e} \bigg|_{h_{e,k}} \right) u_{e,k} + \left(\frac{\partial u_{e,k}}{\partial P_e} \bigg|_{h_{e,k}} \right) \rho_{e,k} \right) \dot{P}_e \right.$$
$$\left. + \left(\left(\frac{\partial \rho_{e,k}}{\partial h_{e,k}} \bigg|_{P_e} \right) u_{e,k} + \left(\frac{\partial u_{e,k}}{\partial h_{e,k}} \bigg|_{P_e} \right) \rho_{e,k} \right) \dot{h}_{e,k} \right] \qquad 17$$

$$\left.\frac{\partial u_{e,k}}{\partial P_e}\right|_{h_{e,k}} = \frac{-1}{\rho_{e,k}} + \frac{P_e}{\rho_{e,k}^2}\left.\frac{\partial \rho_{e,k}}{\partial P_e}\right|_{h_{e,k}} \tag{18}$$

$$\left.\frac{\partial u_{e,k}}{\partial h_{e,k}}\right|_{P_e} = 1 + \frac{P_e}{\rho_{e,k}^2}\left.\frac{\partial \rho_{e,k}}{\partial h_{e,k}}\right|_{P_e} \tag{19}$$

$$\dot{U}_{e,k} = V_{e,k}\left[\left(\left(\left.\frac{\partial \rho_{e,k}}{\partial P_e}\right|_{h_{e,k}}\right)\left(u_{e,k} + \frac{P_e}{\rho_{e,k}}\right) - 1\right)\dot{P}_e \right.$$
$$\left. + \left(\left(\left.\frac{\partial \rho_{e,k}}{\partial h_{e,k}}\right|_{P_e}\right)\left(u_{e,k} + \frac{P_e}{\rho_{e,k}}\right)\rho_{e,k}\right)\dot{h}_{e,k}\right] \tag{20}$$

$$\dot{U}_{e,k} = V_{e,k}\left[\left(\left(\left.\frac{\partial \rho_{e,k}}{\partial P_e}\right|_{h_{e,k}}\right)h_{e,k} - 1\right)\dot{P}_e + \left(\left(\left.\frac{\partial \rho_{e,k}}{\partial h_{e,k}}\right|_{P_e}\right)h_{e,k} + \rho_{e,k}\right)\dot{h}_{e,k}\right] \tag{21}$$

$$\dot{m}_{e,k} = V_{e,k} \cdot \dot{\rho}_{e,k} \tag{22}$$

$$\dot{m}_{e,k} = V_{e,k}\left[\left(\left.\frac{\partial \rho_{e,k}}{\partial P_e}\right|_{h_{e,k}}\right)\dot{P}_e + \left(\left.\frac{\partial \rho_{e,k}}{\partial h_{e,k}}\right|_{P_e}\right)\dot{h}_{e,k}\right] \tag{23}$$

$$E_{w,k} = (C_P\rho V)_w T_{w,k} \tag{24}$$

$$\dot{E}_{w,k} = (C_P\rho V)_w \dot{T}_{w,k} \tag{25}$$

A nonlinear state space form Equation 26 could be used to describe the entire model. This contains *2n+1* states (Enthalpy of *n* regions + Wall Temperature of *n* regions + Pressure across the heat exchanger). These are contained in the state vector *x*, as expressed in Equation 27. *u* and *y* are the input and output vectors described in Equations 28 and 29 respectively. The matrix $Z(x,u)$ consisting of the nonlinear

differential Equations (Equation 30) has all its elements listed in Equations 31 through 45. The matrix $f(x, u)$ is presented in Equation 45.

$$Z(x, u) . \dot{x} = f(x, u) \tag{26}$$

$$x = [\ P_e \quad h_{e,1} \quad \cdots \quad h_{e,k} \quad \cdots \quad h_{e,n} \quad T_{w,1} \quad \cdots \quad T_{w,k} \quad \cdots \quad T_{w,n} \ ]^T \tag{27}$$

$$u = [\ \dot{m}_{in} \quad \dot{m}_{out} \quad h_{in} \quad T_{a,in} \quad \dot{m}_{air} \ ]^T \tag{28}$$

$$Z(x, u) = \begin{bmatrix} Z_{11} & Z_{12} & 0 \\ Z_{21} & Z_{22} & 0 \\ 0 & 0 & Z_{33} \end{bmatrix}_{(2n+1) X (2n+1)} \tag{29}$$

$$Z_{11} = \begin{bmatrix} Z_{11}^1 \\ \vdots \\ Z_{11}^k \\ \vdots \\ Z_{11}^n \end{bmatrix}_{nX1} \tag{30}$$

$$Z_{11}^1 = \left. V_{e,1} \frac{\partial \rho_{e,1}}{\partial P_e} \right|_{h_{e,1}} (h_{e,1} - h_1) - V_{e,1} \tag{31}$$

$$Z_{11}^k = \left. V_{e,k} \frac{\partial \rho_{e,k}}{\partial P_e} \right|_{h_{e,k}} (h_{e,k} - h_k) - V_{e,k} +$$

$$(h_{e,k} - h_k) \left(\left. (V_{e,1} \frac{\partial \rho_{e,1}}{\partial P_e} \right|_{h_{e,1}} + \cdots + \left. V_{e,k-1} \frac{\partial \rho_{e,k-1}}{\partial P_e} \right|_{h_{e,k-1}} \right) \tag{32}$$

$$Z_{11}^n = \left. V_{e,n} \frac{\partial \rho_{e,n}}{\partial P_e} \right|_{h_{e,n}} (h_{e,n} - h_n) - V_{e,n}$$

$$+ (h_{e,n} - h_{out}) \left(\left. (V_{e,1} \frac{\partial \rho_{e,1}}{\partial P_e} \right|_{h_{e,1}} + \cdots \right. \tag{33}$$

$$\left. + \left. V_{e,n-1} \frac{\partial \rho_{e,n-1}}{\partial P_e} \right|_{h_{e,n-1}} \right)$$

$$
Z_{12} = \begin{bmatrix} Z_{12}^{11} & 0 & \cdots & 0 & 0 \\ \vdots & & & & \vdots \\ Z_{12}^{k1} & \cdots & Z_{12}^{k(k-1)} & Z_{12}^{kk} & 0 \\ \vdots & & & \ddots & \vdots \\ Z_{12}^{n1} & \cdots & & Z_{12}^{n(n-1)} & Z_{12}^{nn} \end{bmatrix}_{nXn}
\qquad 34
$$

$$
Z_{12}^{11} = V_{e,1} \left. \frac{\partial \rho_{e,1}}{\partial P_e} \right|_{h_{e,1}} (h_{e,1} - h_1) + V_{e,1}\rho_{e,1}
\qquad 35
$$

$$
Z_{12}^{k1} = (h_{k-1} - h_k)V_{e,1} \left. \frac{\partial \rho_{e,1}}{\partial h_{e,1}} \right|_{P_e}
\qquad 36
$$

$$
Z_{12}^{k(k-1)} = (h_{k-1} - h_k)V_{e,k-1} \left. \frac{\partial \rho_{e,k-1}}{\partial h_{e,k-1}} \right|_{P_e}
\qquad 37
$$

$$
Z_{12}^{kk} = \left(h_{e,k} - h_k \right)V_{e,k} \left. \frac{\partial \rho_{e,k}}{\partial h_{e,k}} \right|_{P_e} + V_{e,k}\rho_{e,k}
\qquad 38
$$

$$
Z_{12}^{n1} = (h_{n-1} - h_n)V_{e,1} \left. \frac{\partial \rho_{e,1}}{\partial h_{e,1}} \right|_{P_e}
\qquad 39
$$

$$
Z_{12}^{n(n-1)} = (h_{n-1} - h_n)V_{e,n-1} \left. \frac{\partial \rho_{e,n-1}}{\partial h_{e,n-1}} \right|_{P_e}
\qquad 40
$$

$$
Z_{12}^{nn} = \left(h_{e,n} - h_n \right)V_{e,n} \left. \frac{\partial \rho_{e,n}}{\partial h_{e,n}} \right|_{P_e} + V_{e,n}\rho_{e,n}
\qquad 41
$$

$$
Z_{21} = \left[V_{e,1} \left. \frac{\partial \rho_{e,1}}{\partial P_e} \right|_{h_{e,1}} + \cdots + V_{e,n} \left. \frac{\partial \rho_{e,n}}{\partial P_e} \right|_{h_{e,n}} \right]_{1X1}
\qquad 42
$$

$$
Z_{22} = \left[V_{e,1} \left. \frac{\partial \rho_{e,1}}{\partial h_{e,1}} \right|_{P_e} \cdots V_{e,n} \left. \frac{\partial \rho_{e,n}}{\partial h_{e,n}} \right|_{P_e} \right]_{1Xn}
\qquad 43
$$

$$Z_{33} = diag\{|(C_P \rho V)_{w,1} \quad \cdots \quad (C_P \rho V)_{w,n}|\} \qquad\qquad 44$$

$$f(x,u) = \begin{bmatrix} \dot{m}_{in}(h_{in} - h_1) + \alpha_{i,1}A_{i,1}(T_{w,1} - T_{r,1}) \\ \vdots \\ \dot{m}_{in}(h_{k-1} - h_k) + \alpha_{i,k}A_{i,k}(T_{w,k} - T_{r,k}) \\ \vdots \\ \dot{m}_{in}(h_{n-1} - h_{out}) + \alpha_{i,n}A_{i,n}(T_{w,n} - T_{r,n}) \\ \dot{m}_{in} - \dot{m}_{out} \\ \alpha_{o,1}A_{o,1}(T_{a,1} - T_{w,1}) - \alpha_{i,1}A_{i,1}(T_{w,1} - T_{r,1}) \\ \vdots \\ \alpha_{o,k}A_{o,k}(T_{a,k} - T_{w,k}) - \alpha_{i,k}A_{i,k}(T_{w,k} - T_{r,k}) \\ \vdots \\ \alpha_{o,n}A_{o,n}(T_{a,n} - T_{w,n}) - \alpha_{i,n}A_{i,n}(T_{w,n} - T_{r,n}) \end{bmatrix}_{(2n+1)X1} \qquad 45$$

Empirical Compressor Map:

```
load FluidProp_R410a_v4

load Data

% Store the selected range of data in new variables

% MDOT = mass flow rate

% V = Volume

% RPM = Speed of the compressor

% TKRI = Refrigerant temperature at the inlet of the compressor

% TKRO = Refrigerant temperature at the outlet of the compressor

% PKI = Pressure at the inlet of the compressor

% PKO = Pressure at the outlet of the compressor

% PO = valve outlet pressure

% EEV = valve command signal

MDOT = Exp2.E_rm(1:16000);

V = 1.5*3.042e-5;

RPS = (1500*Exp2.Comp(1:16000))./60;

RPM = 1500*Exp2.Comp(1:16000);

TKRI = Exp2.Tero(1:16000);

TKRO = Exp2.Tcri(1:16000);

PKI = Exp2.Pero(1:16000);

PKO = Exp2.Pcro(1:16000);

Pratio = PKO./PKI;
```

```
HIN  = qinterp2(FluidProp.T_mg_pt,FluidProp.P_mg_pt,FluidProp.H_pt_g,TKRI,PKI);

HOUT=

qinterp2(FluidProp.T_mg_pt,FluidProp.P_mg_pt,FluidProp.H_pt_g,TKRO,PKO);

% Calculate the inlet fluid density

RHO_K=

qinterp2(FluidProp.H_mg_ph,FluidProp.P_mg_ph,FluidProp.Rho_ph_g,HIN,PKI);

% Calculate the volumetric efficiency

ETA_V = MDOT./(V*RPS.*RHO_K);

% Calculate the inlet fluid entropy

S = qinterp2(FluidProp.H_mg_ph,FluidProp.P_mg_ph,FluidProp.S_ph_g,HIN,PKI);

% Calculate the isentropic outlet fluid enthalpy

HOUTS = qinterp2(FluidProp.S_mg_ps,FluidProp.P_mg_ps,FluidProp.H_ps_g,S,PKO);

% Calculate the adiabatic efficiency

ETA_A = (HOUTS - HIN)./(HOUT-HIN);

% Form input matrix X, assuming a model structure

X = [RPM Pratio];

% Find model coefficients using left matrix division (approximate matrix inverse)

a = X\ETA_A;

% Find model coefficients using left matrix division (approximate matrix inverse)

a1 = X\ETA_V;

% Clear the variables used for map generation

clear Pi
```

```matlab
clear Po

clear rpm

clear eta_v_map

clear eta_a_map

% Define input variable vectors

Pr = 1:0.1:5.1;

rpm = 0:46.6572:1959.6;

% Generate the lookup table using a for loop for each input, Equation should match the

model structure chosen for the X matrix

for c1 = 1:length(rpm)

for c2 = 1:length(Pr)

eta_v_map(c1,c2) = a1(1)*rpm(c1) + a1(2)*Pr(c2);

eta_a_map(c1,c2) = a(1)*rpm(c1) + a(1)*Pr(c2);

%if the value of either eta_v or eta_a is less than zero because of the polynomial fit,

assume it to be a very small value, say 0.01.

end

end

% Store the input vectors and lookup table array in a structure

CompProptrane.rpm = rpm;

CompProptrane.Pr = Pr;

CompProptrane.eta_v = eta_v_map;

CompProptrane.eta_a = eta_a_map;
```

Empirical Valve Map:

```
load FluidProp_R410a_v4

load Data

% Store the selected range of data in new variables

% MDOT = mass flow rate

% PI = valve inlet pressure

% PO = valve outlet pressure

% EEV = valve command signal

PI = Datafull.Pcro;

PO = Datafull.Pero;

deltaP = PI-PO;

MDOT = Datafull.E_rm;

EEV = Datafull.EEV;

% Calculate the inlet fluid density, assuming the inlet fluid is saturated vapor

RHO_V = interp1(FluidProp.Psat,FluidProp.Rhof,PI);

% Calculate the flow coefficient (valve area * discharge coefficient)

CF = MDOT./(sqrt(RHO_V.*(deltaP)));

% Form input matrix X, assuming a model structure

X = [ones(size(MDOT)) EEV deltaP EEV.*deltaP EEV.^2];

% Find model coefficients using left matrix division (approximate matrix inverse)

a = X\CF;
```

```
% Clear the variables used for map generation

clear Pi

clear Po

clear eev

clear Cf_map

% Define input variable vectors

dP = 0:8.057:1700;

eev = 0:0.1:21;

% Generate the lookup table using a for loop for each input, Equation should match the

model structure chosen for the X matrix

for c1 = 1:length(eev)

for c2 = 1:length(dP)

Cf_map(c1,c2) = a(1) + a(2)*eev(c1) + a(3)*dP(c2) ...

+ a(4)*eev(c1)*dP(c2)+ a(5)*eev(c1)^2;

end

end

% Store the input vectors and lookup table array in a structure

ValvePropnew.dP = dP;

ValvePropnew.u = eev;

ValvePropnew.Cf_v = Cf_map;
```

VITA

Name:	Balakrishna Ayyagari
Address:	3123 TAMU Department of Mechanical Engineering, Texas A&M University, College Station, TX 77843-3123
Email Address:	balakrishna_ayyagari@yahoo.com
Education:	B. Tech., Mechanical Engineering, Jawaharlal Nehru Technological University, 2008 M.S., Mechanical Engineering, Texas A&M University, 2011